

University of Nebraska - Lincoln

DigitalCommons@University of Nebraska - Lincoln

Mechanical (and Materials) Engineering --
Dissertations, Theses, and Student Research

Mechanical & Materials Engineering,
Department of

Summer 8-28-2022

SCALING CELLULAR AGRICULTURE PRODUCTION WITH PHOTOLITHOGRAPHY: A STUDY ON CURING AND DEGRADATION

Alexis Garrett

University of Nebraska-Lincoln, alexis.garrett@huskers.unl.edu

Follow this and additional works at: <https://digitalcommons.unl.edu/mechengdiss>



Part of the [Materials Science and Engineering Commons](#), and the [Mechanical Engineering Commons](#)

Garrett, Alexis, "SCALING CELLULAR AGRICULTURE PRODUCTION WITH PHOTOLITHOGRAPHY: A STUDY ON CURING AND DEGRADATION" (2022). *Mechanical (and Materials) Engineering -- Dissertations, Theses, and Student Research*. 182.

<https://digitalcommons.unl.edu/mechengdiss/182>

This Article is brought to you for free and open access by the Mechanical & Materials Engineering, Department of at DigitalCommons@University of Nebraska - Lincoln. It has been accepted for inclusion in Mechanical (and Materials) Engineering -- Dissertations, Theses, and Student Research by an authorized administrator of DigitalCommons@University of Nebraska - Lincoln.

**SCALING CELLULAR AGRICULTURE PRODUCTION WITH
PHOTOLITHOGRAPHY: A STUDY ON CURING AND DEGRADATION**

by
Alexis Dawn Garrett

A THESIS

Presented to the Faculty of
The Graduate College at the University of Nebraska
In Partial Fulfillment of Requirements
For the Degree of Master of Science

Major: Mechanical Engineering and Applied Mechanics

Under the Supervision of Professor Michael P. Sealy

Lincoln, Nebraska

August, 2022

SCALING CELLULAR AGRICULTURE PRODUCTION WITH PHOTOLITHOGRAPHY: A STUDY ON CURING AND DEGRADATION

Alexis Garrett, M.S.

University of Nebraska, 2022

Advisor: Michael P. Sealy

The coronavirus pandemic caused significant strain on the global food economy, and a gap in safeguarding a resilient food system and corresponding infrastructure was highlighted. Over the last few decades, cell-based foods are one potential source to diversify the food production system to become more resilient. Current techniques are far from the required scalability and cost efficiency required to impact the current agriculture system. Significant research has been conducted in cellular biology to improve upon the system currently in use for biomedical purposes, but much of the gap between biomedicine and food science has yet to be closed. This is partially due to a hesitancy of the existing food system to adapt to include alternative protein production methods, such as cellular agriculture. To meet the requirements for full production in cellular agriculture, a multi-disciplinary approach is required. New questions and understandings between different concepts, such as texture and cooking, need to be identified and how they correlate with cellular behavior and taste. Preliminary steps in this process are to gather resources, pose questions, and build standardization for these products to define success. This work focuses on understanding and developing photolithographic systems for scalable cellular agriculture. There were two specific research directions: 1) a

traditional photolithography printing system was improved upon for mass manufacturing purposes and 2) mechanical analysis and degradation of key potential photolithographic biomaterials were tested for a food product. A novel digital rotational ultraviolet manufacturing (DRUM) process was developed, and initial photolithographic printing tests were carried out. GelMA hydrogels were tested in uniaxial compression and compared to a range of meat samples at 20°C using constant displacement speed control. The results showed effective mimicry under the defined environment to that of raw scallops, but not of higher order constructs. A soy-based resin was also tested in degradation 37°C for 0 to 28 days in phosphate buffered solution and ethanol solutions. Degradation was successfully mapped via thermomechanical means in dynamic mechanical analysis. Stability of the material was verified upon addition of EBC-1 enzyme. Initial values for the mechanical behavior of pure soya scaffolds at 100% density were too stiff and unable to match desired findings in literature. The achieved results showed promise as a proof of concept for this methodology and emphasizes the importance of standardization of results, ultimately leading to the conclusion that the requirements for these products will likely require complex modular, multi-step, multi-material systems at scale.

DEDICATION

I dedicate this thesis to my mother, Joan Kamerzell, for being steadfast support through my entire education and career endeavors. Without her I would not be the woman I am today.

ACKNOWLEDGEMENTS

The list of people who have helped make this possible is exhaustive. First, I would like to thank my advisors, Dr. Michael Sealy and Laurent Delbreilh for their guidance throughout my graduate studies. I would like to acknowledge my committee members for their contributions to shape the intellectual merit of this work: Michael P. Sealy, Laurent Delbrieh, Mehrdad Negahban, and Nicolas Delpouve. Thank you to Dr. Juan Segurola of 3DResyns for collaborating and sourcing some of the materials used in these studies. Thank you also to Dr. David Kaplan and Andrew Stout of Tufts University for boundless resources in the cellular agriculture field and additionally supplying cells for studies. Thank you to Dr. Ali Tamayol, Jacob Quint, and Carina Russell for giving me insight and direct hands-on experience in cell studies in the beginnings of this endeavor. Thank you also to Dr. Jeffrey Shield and the additional work of Arian Jaber and Auston Viotto through the Additive Manufacturing course that allowed for the development of DRUM.

Thank you also to my fellow lab mates who made the world a little brighter when all seemed particularly bleak. Thank you to the Wilson family for being true friends when friends were needed most, and my family for always being there with love and inspiring me to lead by example. Thank you to Antonella Esposito for being an invaluable resource and dear friend to me and helping to reinvigorate my confidence and belief in the work-including the importance and beauty in academic research. I would like to also thank Sam for the support through some of the hardest nights of my career, and the constant encouragement given throughout the process.

I would like to acknowledge the GS-MES program at the University of Rouen for providing financial, research, and professional support, without which my studies in Rouen would have been far more difficult. Finally, I would like to thank the New Harvest community for acting as a family and taking me into the ranks. With their financial, intellectual, and personal aspirational support, I was able to pursue ideas otherwise not accessible to me. They have provided so much for the endeavors described in this body of work and have been an outstanding organization to work with. My hope is to stay connected to this organization for life and watch it grow and change the world as it changed mine.

CONTENTS

ABSTRACT.....	i
DEDICATION.....	iii
ACKNOWLEDGEMENTS.....	iv
LIST OF TABLES.....	viii
LIST OF FIGURES.....	ix
CHAPTER 1: CELLULAR AGRICULTURE, ITS USES, AND THE HURDLES IN MATERIALS AND MECHANICS UNDERSTANDING	1
1.1 The Food Horizon Dilemma: What are the Stakes?	1
1.2 What is Cellular Agriculture?	2
1.3 The Materials Dilemma: What are the Steaks?.....	4
1.5 Research Objectives.....	6
1.6 Organization of Thesis.....	6
CHAPTER 2: REVIEW OF REQUIREMENTS AND CURRENT METHODS OF ENGINEERED TISSUE MANUFACTURING.....	8
2.1 Tissue Engineering Considerations.....	8
2.1.1 Skeletal Muscle Anatomy	8
2.1.2 Cell Culture and Adhesion.....	8
2.2 Scaffold Manufacturing Processes.....	10
2.2.1 Hydrogel	10
2.2.2 Fiber	15
2.3 Commercial Equipment for Bioprinting.....	18
2.3.1 Bioprinter 1 – Allevi 2	18
2.3.2 Bioprinter 2 – Lumen X.....	19
2.3.3 Bioprinter 3 – Holograph X.....	20
CHAPTER 3: BUILDING DRUM AND INITIAL TESTING	21
3.1 Motivation.....	21
3.2 Design Requirements	22
3.2.1 Cell-Culture Compatibility	22
3.2.2 Print Quality.....	23
3.2.3 Adjustable Material Properties.....	24
3.3 Design Process.....	24
3.3.1 Design Option 1: Upward-Motion Collector Plate (UMCP)	25

3.3.3	Design Option 3: Rotational Volumetric Printing (RVP)	29
3.4	Evaluation of Methods	31
3.4.1	Evaluation Criteria	31
3.4.2	Weight Factors	35
3.4.3	Pugh Matrix Results	36
3.5	Final Design: Digital Rotational Ultraviolet Manufacturing (DRUM).....	38
3.5.1	Key Features	40
3.5.2	Advantages.....	42
3.5.3	Disadvantages	45
3.6	Manufacturing.....	46
3.6.1	Materials	47
3.6.2	Required Component Features.....	47
3.6.3	Cost Analysis	51
3.7	Testing and Evaluation	52
3.8	Discussion.....	55
CHAPTER 4: BIOMATERIALS STUDY FOR PHOTOLITHOGRAPHIC TISSUE ENGINEERING APPLICATIONS		57
4.1	Introduction.....	57
4.2	Motivation.....	58
4.3	GelMA Compression Study	59
4.3.1	Materials and Methods.....	59
4.3.2	Results.....	62
4.3.3	Summary	65
4.4	Bio Soya Resin Degradation.....	66
4.4.1	Materials and Methods.....	67
4.4.2	Results.....	74
4.4.3	Summary	82
4.5	Discussion.....	83
4.6	Conclusions.....	85
CHAPTER 5: SUMMARY, CONCLUSIONS, AND FUTURE WORK		87
5.1	Summary	87
5.2	Conclusions.....	88
5.3	Future Works for the Field.....	89
REFERENCES		92
APPENDIX.....		99
A1.	Bill of Materials	99
A2.	Code	102

LIST OF TABLES

3.1	Pugh matrix iteration 1 with flooded laid fiber network (FLF) as the control	36
3.2	Pugh matrix iteration 2 with upward motion collector plate (UMCP) as the control	37
3.3	Pugh matrix iteration 3 with rotational volumetric printing (RVP) as the control	38
4.1	Sample Nomenclature for GelMA compression results	65
4.2	Nomenclature for non-enzyme soya resin samples	69
4.3	List of tests and time points utilized in degradation analysis	70
4.4	Key Moduli and Peak Relaxation for Aged Samples	80

LIST OF FIGURES

2.1	(a) Visual schematic of fundamental photolithography, (b) visual schematic of extrusion-based hydrogel bioprinting, (c) depiction of common scaffold fabrication process via molding and leaching.	13
2.2	(a) Visual schematic of fundamental electrospinning concept and (b) visual schematic of immersion rotary jet spinning concept.	17
2.3	(a) Allevi 2 printer by Allevi, (b) LumenX SLA printer by CellInk, (c) HolographX holographic volumetric printer by CellInk.	19
3.1	Proposed schematic of design iteration 1, the upward motion collector plate system.	26
3.2	Proposed schematic of design iteration 2, the flooded laid fiber network system.	28
3.3	Proposed schematic of design iteration 2, the rotational volumetric printing system.	30
3.4	(a) CAD model of Digital Rotational Ultraviolet Manufacturing (DRUM). (b) Image of the DRUM printer during operation. (c) Layer cross-sections for hydrogel (blue) and electrospun fiber sheets (orange) for layer-by-layer and radial-layer prints.	39
3.5	DLP printed resin-based structures: (a) patterns of the projected sketch; (b) printed structures: (i) B9 printed (ii, iii, iv, v) DRUM printed. Scale bar: b, 25 mm.	55
4.1	Depiction of the Mix, Cure, and Test of compression samples.	62
4.2	Variation of hydrogel concentrations and treatment. The engineering stress strains plotted, where the adjustment in (a) curing times, (b) GelMA concentration, and (c) tartrazine concentration are identified.	63
4.3	GelMA and Meat Tissue. Engineering stress-strain curves of GelMA 7% with 0-tartrazine compared with (a) all meat tissue samples tested, and (b) an isolated comparison with scallops for further discussion.	64
4.4	Schematic of degradation in which (1) the functionalized photocrosslinkable resin and enzyme are mixed, (2) the material is exposed to UV, creating radicals in the material. (3) These radicals initiate crosslinking between the functionalized molecules. (4) Upon	67

submersion in solution, the material degrades with the enzymes serving as a catalyst to the degradation of bonds.

- 4.5** Chemical bonding evolution throughout crosslinking process. 76
- 4.6** DMA of soya with additive enzyme EBC-1 and swelling of soya in solution. (a) storage and loss moduli and $\tan(\delta)$ of biosoya 1 resin with (blue) and without (red) EBC-1 enzyme. (b) graphed swelling in each solution represented as %w of solution absorbed to sample weight. 77
- 4.7** DMA of soya with additive enzyme EBC-1 (a) DMA storage and loss moduli evolution due to ethanol aging, with no aging (black) as reference. (b) DMA storage and loss moduli evolution due to PBS aging with no aging (green) as reference 78
- 4.8** DSC Analysis of soya degradation combined graph, normalized 80

CHAPTER 1: CELLULAR AGRICULTURE, ITS USES, AND THE HURDLES IN MATERIALS AND MECHANICS UNDERSTANDING

1.1 The Food Horizon Dilemma: What are the Stakes?

In a span of 55 years from 1961 to 2016, the global population grew from three to seven billion people, paired with a growth in meat consumption per capita by 75%¹. These compounding growths apply a strain to agriculture's traditional methods for matching this new meat demand. The key constraints for this optimization problem are in land, water and the usage of energy, with an added consideration in greenhouse gas emissions which is experiencing significant regulatory pushback in recent years. Some studies have identified cellular agriculture as a potential avenue to increase the efficiency of the production of meat products by some significant margins, with 99% less land usage, 82-96% less water usage, and 78-96% less greenhouse gas emissions², while others are less optimistic of this field's capability³.

Currently, genetically modified crops and selective bred livestock are used to increase yield to match the requirements, but have physical limits to their benefits. The term genetic modification already holds with it strong controversy in the public eye contemporarily, and has been used as a fear mongering phrase for competitive brands who may use these products. Scientifically, these products typically serve no identified health hazard to the consumer⁴. Without genetic modification, our current food production would likely not accommodate for nutritional requirements. One of the most

common examples of this is selective breeding of livestock to be larger, and grow to maturity at a quicker rate, but can come at a cost of the health and welfare of the animals.⁵ The speed at which these animals or crops can be grown to maturity is still limited to the efficiency of energy and food used in the system. A very famous quote from Winston Churchill on the matter brings a challenge to our current thinking, postulating that someday “we shall escape the absurdity of growing a whole chicken in order to eat the breast of wing, by growing these parts separately under a suitable medium.”

With the onset of a global pandemic which created halts to major production lines and reduced food security with contaminations at traditional meat processing plants, it is imperative to investigate the options for improving upon current food manufacturing methods with disruptive innovations. These new methods can be designed from the ground up with our current understanding of food, climate, socioeconomics, and safety in mind, rather than tweaking the current agricultural methods and hoping for the best. The answer to this dilemma may in fact be cellular agriculture.

1.2 What is Cellular Agriculture?

Cellular agriculture is a field in its infancy with the goal to accomplish Churchill’s vision of the future- producing meat and other animal-based products like milk or eggs without the animal itself. This industry has brought in funding in relatively large sums in the private sector but not as much in the federal or governmental backing. Only recently has the United States funding agencies begun investment in this field, with an initial USDA AFRI grant award of \$10 million for 2022 to 2026⁶. These investments

are made with the intention to improve upon current technology in development, for example the ability to create a ground beef product for approximately \$100 or less rather than the \$280,000 in 2013⁷. This trend is promising for these ground products to hit the consumer market soon as regulatory measures are passed, but the higher order textures, present in products such as a beef steak, have yet to be efficiently achieved or scaled to the same production level as that of the ground cellular products.

Current manufacturing methods for cultured proteins are slow, expensive, and unable to achieve textures beyond conventional ground meats. Production rates of cultured proteins using existing biomanufacturing tools are insufficient for reaching economies of scale capable of competing with animal-based production. To address challenges related to feeding the global population, a convergent approach between manufacturing, tissue engineering, and food science is needed to enable new manufacturing knowledge to address the challenge of rapid production of textured constructs. Current products are costly and unable to achieve textures beyond conventional ground meats (*e.g.*, hamburger or hotdog). Significant emphasis has been placed on development of cell lines, but a lacking endeavor is that of the materials behavior of the potential scaffolding material during the biomaturation and cooking stages³.

A strong argument against the efficacy of cellular agriculture is the need to drive down production costs to around the same as that of current meat products³. One identifiable opportunity to develop these methods while attempting to bring down costs is in process development for production in remote locations, defined by the inhospitable land for livestock rearing or inability to store mass amounts of food for extended periods of time. Initial possible locations that could benefit from these developed technologies

include submarines, increasing submersion time to six months rather than three to increase military readiness; other-planet colonization where raising livestock is impossible; or deserts where water is not in high supply. Once an initial methodology is developed, these scenarios could serve as ideal testbeds for the efficacy of the technology, allowing the field to grow and accommodate for scale and cost.

1.3 The Materials Dilemma: What are the Steaks?

One of the biggest concerns with regards to the development of cellular agriculture is in the health and safety of the process and the products. Much of this field and the technologies within is undiscovered or untested. This lack of knowledge causes skepticism in the field and without proper branding and understanding of the products- regardless of how perfect the technology is- it still may not be adopted by the public, similar to the term “GMO” or Soylent. So how is this knowledge gap closed, both in the field and between producer and consumer? Many of the start-ups and non-profits in this industry have been in collaborations to define the strategy for achieving safety and eventual FDA approval⁸. This collaboration is a good sign and should improve the speed at which these are developed, but additional work needs to be done on the actual product side as well, and some of these technologies can be seen in biomedicine as well as cellular agriculture. First and foremost, edibility and understanding how the body will metabolize the product is crucial for success. After this come taste, cost, nutrition, and actual demand for primary cultural acceptance. Finally for true realization of benefits, improved nutrition, accessibility, and safety as well as reduced use of resources and overall effect on climate should be the goal.

Though bioprinters and some biomaterials are commercially available, models have not been developed that allow for significant tailoring of the production methodology. These are especially lacking with respect to seamless scale-up. Hypothesized methods for improving upon the system can be split into cellular biology, texture, or scale-up in particular, and all have interconnections that are important for implementation. Scale-up is mostly designated to development for cellular agriculture, but innovations in cellular biology and texture are required to be able to improve upon the scalability and the industry horizon.

Significant emphasis has been placed in the field of study on improving the cellular biology component of these systems. Recently, new media that don't rely on animal products have been developed⁹, efficient design of experiments has been implemented to increase the speed at which these media formulations are optimized¹⁰, and cell lines themselves have been modified to increase protein or lipid production, improving nutrition and eventual taste of these cell systems¹¹. On the side of texture, some have proposed using natural materials as scaffolds for cells that provide similar textures such as jackfruit¹². Others have identified potential materials processing and combinations to create the same desired results¹³, but these are all significantly limited in the testing methodologies used in each. Though they all contain great promise for approaches to scale-up both of product size and of process, there is yet to be a standardization of the success criteria and how to test them. As a simple example, very few test these materials or methods among a range of temperatures, which is crucial in understanding how these food stuffs will handle being cooked.

1.4 Research Objectives

The aim of this research is to bring to light these considerations and the need for standardization and understanding, with a focus on scale-up and texture considerations in manufacturing and materials selection. This was pursued in two primary objectives. The first objective was to investigate current biomanufacturing methods and suggest a novel process for improved speed of production. The second main objective was to identify and characterize two potential materials to be used in this system. In this objective, key considerations are emphasized for further development of this system as well as others aiming to achieve the same goal. In large part, this report should serve as one bridge between multiple fields of thought in materials characterization and processing - from manufacturing to cellular biology to materials and food sciences.

1.5 Organization of Thesis

This thesis serves as a comprehensive collection of studies and knowledge gathered while pursuing the above defined goals and objectives. [Chapter 1](#) provides an introduction to cellular agriculture as a field of study as well as the place this research holds within it. [Chapter 2](#) delves into further detail the requirements for biomanufacturing processes, including current methods and key considerations for cellular biology. [Chapter 3](#) packages the design and testing processes of the proposed manufacturing method and lays out the further work needed to develop this to completion. [Chapter 4](#) serves as an in-depth report of the materials characterization undergone for this application and the insights gathered throughout the process. Finally, [Chapter 5](#) provides a final summary and critical analysis of the conducted research, and identifies potential paths forward in

the development of cellular agriculture into an effective method for sourcing food products.

CHAPTER 2: REVIEW OF REQUIREMENTS AND CURRENT METHODS OF ENGINEERED TISSUE MANUFACTURING

2.1 Tissue Engineering Considerations

2.1.1 Skeletal Muscle Anatomy

Skeletal or striated muscle consists of bundles of thousands of muscle fibers connected via the extracellular matrix or ECM that serves as a natural scaffold for the muscle tissue¹⁴. This extracellular matrix- primarily made up of collagen, enzymes, and glycoproteins- is crucial to cell adhesion and migration within the tissue and helps to regulate the cellular growth, metabolism and differentiation exhibited by the attached cells¹⁵. In addition, marbling of muscle tissue with intermittent fatty regions further increases the complexity of the structure, both in material composition and regional structural properties¹⁶. This complex material and structural variation must be mimicked in a cultivated meat to achieve higher order textures within the product.

2.1.2 Cell Culture and Adhesion

In order to recreate the structure of skeletal muscle *in vitro*, the cellular environment of the tissue must be mimicked. This cellular environment defines the interactions between the cells and the material of the scaffold as well as the interactions between cells dispersed in the scaffold. For a scaffold to be effective for tissue engineering, it must contain bonding moieties that the cells can adhere to. Cells,

especially those found in skeletal muscle tissue, have significantly improved proliferation and maturation when under stress. The bonding moieties serve as connection points in which the cell body can adhere. This connection induces minor stresses that help the cells to survive and thrive in the system¹⁷. If these moieties do not exist within the scaffold, the cells will not attach to the scaffold and the ratio of cell death to seeded cells increases significantly.

In addition to the moieties required for adhesion, the scaffold must also have pathways that are perfusable by the cells. If the scaffold is too dense or lacks sufficient pore sizes, the cells will only attach to the surface of the structure, resulting in significant regions of acellular material¹⁸. These pathways also facilitate the movement of nutrients to and waste from the bonded cell sites. Without the waste removal and nutrient supply, areas of high necrosis will occur within the scaffold.

Finally, working alongside the physical architecture, the chemical environment within the scaffold controls the chemical signaling within the scaffold and has a significant impact on the cell to cell and cell to scaffold interactions¹⁹. This chemical environment can be controlled by the material the scaffold is fabricated from as well as the media or additional materials added to the system during the *in vitro* growth of the cell-derived tissue. It is important to understand the base materials used as well as any and all physical or chemical interactions experienced throughout the entire process. Key considerations that are constant in cell culture are the diffusion of media as well as the temperature of 37°C required to keep the cells at their optimal temperature for cellular proliferation²⁰.

2.2 Scaffold Manufacturing Processes

Although basic culturing techniques have been established for the components for tissue engineering and many manufacturing methods for 3-dimensional tissue scaffolds have been developed, these methods are still in their infancy and focus on the cellular behavior rather than the experiential aspects of the tissue construct, such as successfully controlling the directional mechanical behavior or degree of anisotropy within the thick constructs. These methods range widely from scaffoldless systems²¹, three dimensional printable structures, decellularized natural extracellular matrices from plant sources²², and many more novel approaches. This project focuses on developing methods that utilize scaffolds rather than the scaffoldless methods. One method that has been investigated in its ability to control the degree of anisotropy is through an extrusion-based printing of PCL, a medical grade polymer, and the incorporation of intermittent layers of electrospun PCL nanofibers²³. This hybrid technology shows significant potential in giving way to increasing the controllability of the directional mechanical behaviors under loading. Before first determining an ideal method for scaffold production, each of the most common scaffold types and their production methods must first be identified.

2.2.1 Hydrogel

Hydrogels are a commonly studied biomaterial that can comprise both from natural and synthetic material. These hydrogels can either be physically or chemically crosslinked. Physical crosslinking occurs when the material adapts to its physical environment such as a temperature decrease which can force the material to transition from a liquid state to a solid state. Physical crosslinking can be easily reversed if the

temperature is raised once more, which reduces its effectiveness in creating a scaffold to be used at a raised temperature. Chemical crosslinking can be achieved through various methods but typically require a catalyst to be present within the material. Some catalysts will initiate the crosslinking given ample time, whereas other methods may require additional stimuli to initiate the crosslinking. One of the most common chemical crosslinking methods in hydrogel structures is photoinitiated crosslinking in which light, typically UV, is inputted into the material which excites the photo-initiating particles. When these particles are excited, they bombard the hydrogel molecules and induce crosslinking between the molecules. One drawback to the UV curing method for edible purposes is the typically toxic photo-initiator requirement to be completed²⁴.

Synthetic hydrogels generally exhibit structural integrity and geometrical control superior to their natural counterparts²⁵. The most common synthetic hydrogels used in the medical field are polycaprolactone (PCL) or polylactic acid (PLA) based, which are not edible and therefore are not usable for the application desired with this project focus. Natural hydrogels have been developed with a variety of materials. The most common materials are variations of gelatin, silk, agar, and alginate²⁶. These materials do not naturally perform as well as the synthetic materials but are edible and can be tunable to the need of the scaffold. One of the most common methods for tuning these materials is through the functionalization to improve the crosslinking ability. This requires an initial process that will add stronger bonding sites on the material's molecular structure which makes it easier to crosslink between the molecules²⁷. One drawback to the natural materials is the lack of the required bonding moieties in the scaffold for the cells to attach to in the plant-based counterparts. Alginate, although easily mass produced and plant-

based, does not contain the RGD moieties required for the skeletal muscle cells to attach to²⁸. This requires further functionalization of alginate to incorporate these binding moieties to create an acceptable material for scaffold production, which is a tedious and expensive process. Gelatin-based materials, although animal-produced, naturally contain these bonding moieties and show high cellular compatibility and proliferation. A happy medium determined between the two subcategories of natural hydrogels would be ideal to reduce the dependence on animal products but also to ensure that the scaffold is effective for cell-culture.

The most common methods for constructing hydrogel scaffolds are through photolithography, extrusion-based printing, and molding followed by a lyophilization process which removes the water and expands the material due to the freezing and vacuum expansion processes which will increase the pore size.

Photolithography

Photolithography, as depicted in **Figure 2.1a**, utilizes chemical crosslinking and has exhibited high control of the creation of vascular paths within the material²⁹. An architecture is printed layer by layer through exposing a layer in a defined pattern and light intensity for an optimized exposure time. With a longer exposure time, a higher intensity of crosslinking can be achieved, but a lower control of the resolution, as the extended exposure increases the likelihood the light will travel through the material and cure any uncured areas in the previous layer. A drawback to this method is the requirement of a photoinitiator which, as identified previously, can be toxic to the cells and not safe for human consumption. In order for this to be a method compatible for

edible cell culture, further development and testing of edible photoinitiators, such as riboflavin for gelatin-based materials³⁰, must be conducted.

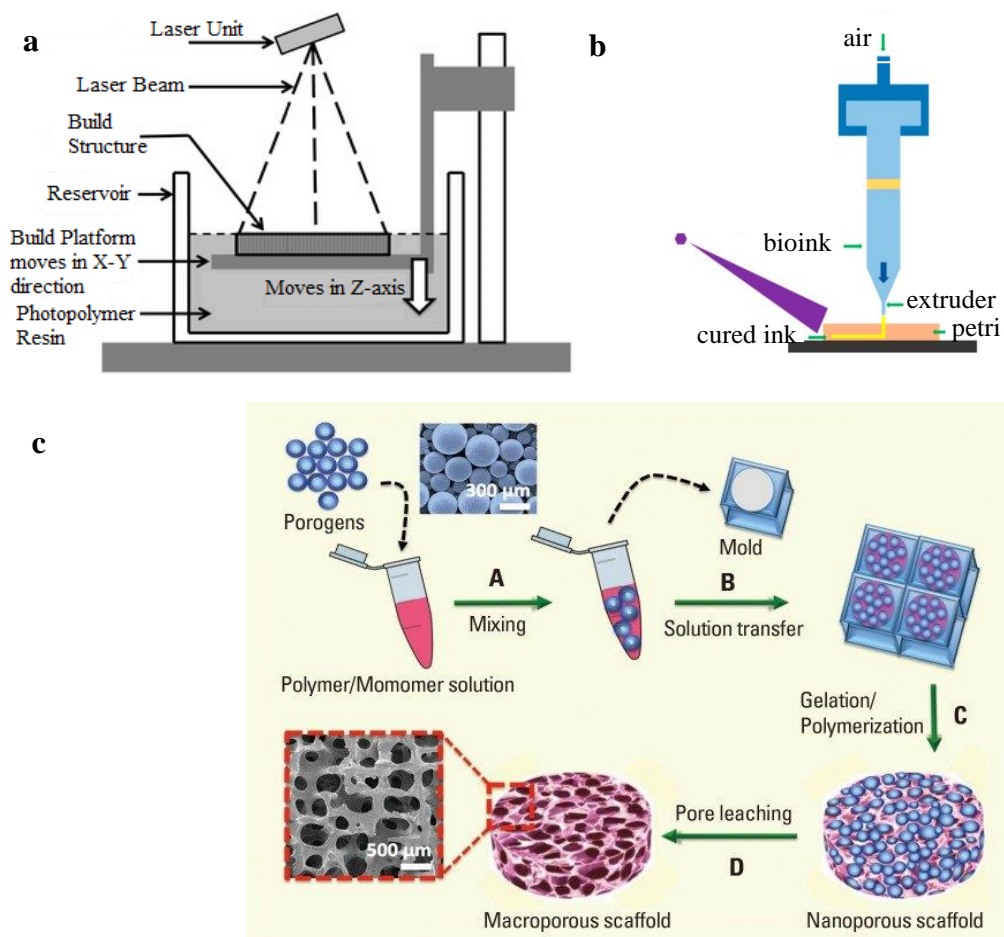


Figure 2.1. (a) Visual schematic of fundamental photolithography³¹, (b) visual schematic of extrusion-based hydrogel bioprinting³², (c) depiction of common scaffold fabrication process via molding and leaching³³.

Extrusion-based

Extrusion-based bioprinting is like that of the highly popular extrusion-based methods for plastic fused filament printing and is depicted in [Figure 2.1b](#). In this process, the hydrogel is extruded through a syringe needle either through pneumatic or

displacement control. This extruded material can either be physically or chemically crosslinked. In the physically crosslinked process, the needle of the syringe is heated past the melting temperature of the hydrogel and upon deposition onto the collection plate it is cooled into a retained shape. In the chemically crosslinked process, the needle does not require heating, but after a layer is deposited, the layer will be subjected to ultraviolet light to cure. Although this method allows for both physical and chemical crosslinking and has high control over material deposition, the resolution of the print possible is restricted to the minimum needle size available for use in printing. Another common pitfall to extrusion-based methods is the natural delamination points created between the layers and the reduced mechanical properties when compared to a part of similar shape that is cast³².

Molded

These hydrogel scaffolds can also be prepared through the use of molds that can be flooded or filled with the hydrogel and crosslinked physically or chemically. This molding process can come in various forms and have benefits for specific purposes. One method that incorporates molding is micro-molding or micro-stamping in which a textured mold or plate is used to add a designed topography to the surface of the mold. This functionalization of the surface, such as the addition of micro-grooves, of the hydrogel affects the bonding behavior of the cells and can increase the rate of maturation of myoblast cells into myotubes, a key milestone in effectively maturing the tissue for mimetic muscle structures³⁴. Another method for creating tissue scaffolds through a molding process is the curing of the hydrogel followed by a lyophilization cycle.

Lyophilization, also known as freeze drying, involves the freezing of the material which expands the water within the molded gel. After complete freezing of the material, it is then attached to a lyophilization apparatus in which a vacuum is pulled on the system and the frozen water is pulled out of the scaffold. In the place of what was previously expanded water, enlarged pores can be found throughout the structure³⁵. This serves as the network in which the cells and other materials can perfuse and is crucial to creating a thicker tissue construct from a molded scaffold.

2.2.2 Fiber

Another common scaffold type used in tissue engineering research is fabricated fiber networks. These fibers have diameters from a few microns to a few nanometers in scale, depending on the forming process, and exhibit potential as a method for creating scaffolds that are mechanically robust³⁶, increase cell differentiation rate³⁷, and are anticipated to be easily scalable to larger systems³⁸. The most common fiber formation methods are as follows:

Electrospinning

Electrospinning, seen in [Figure 2.2a](#), utilizes high voltages to draw a fiber from a solution. As the electrospinning solution, consisting of the material to be spun dispersed within a volatile solvent, is drawn from a syringe through a needle of specified diameter and length, the volatile solvent within the solution is evaporated in its travel from the syringe to the collector plate. This collector plate can be a flat plate, rotating drum, or many other geometrical variations, such as a human ear replica³⁹. This system is highly

complex and consists of many variables to be set to determine the optimal spinning conditions, including ambient temperature and humidity in the room while spinning. This can cause for complexity and significant time consumed in optimization, but the system is capable of drawing fibers consistently on the nano-scale and of varying material compositions⁴⁰. One of the most significant concerns in the ability to utilize this method safely by the average consumer is the high voltage source required to pull the fibers, causing a potential hazard during operation. In addition, these structures are typically too dense for the cells to be able to diffuse through the scaffold, a significant hurdle in the use of electrospun scaffolds for thick construct fabrication. One proposed method for overcoming this thickness hurdle is through separate manufacturing of these scaffolds followed by a stacking procedure to achieve the desired thickness⁴¹. An additional method, that can also be utilized for the following fabricated method, is through the use of critically sublimated carbon dioxide to expand the gaps between the fibers and create a more desired pore size and density⁴².

Immersion rotary jet spinning

Immersion rotary jet spinning is similar to electrospinning as the fibers are pulled from a solution utilizing a physical force within the material. As depicted in **Figure 2.2b**, the force utilized in the rotary jet spinning is centrifugal. This force is induced as the collection bath system rotates at high speeds. Fibers are then pulled from the solution through the fluid motion caused by the presence of the centrifugal motion. This method is able to produce fibers on the micro-scale and at significantly higher rates of production when compared to electrospinning, but the internal structure of the scaffold created

directly after spinning is not highly controlled and would require post-processing to ensure the required pore size or overall material density is low enough for proper cell survival and proliferation⁴³.

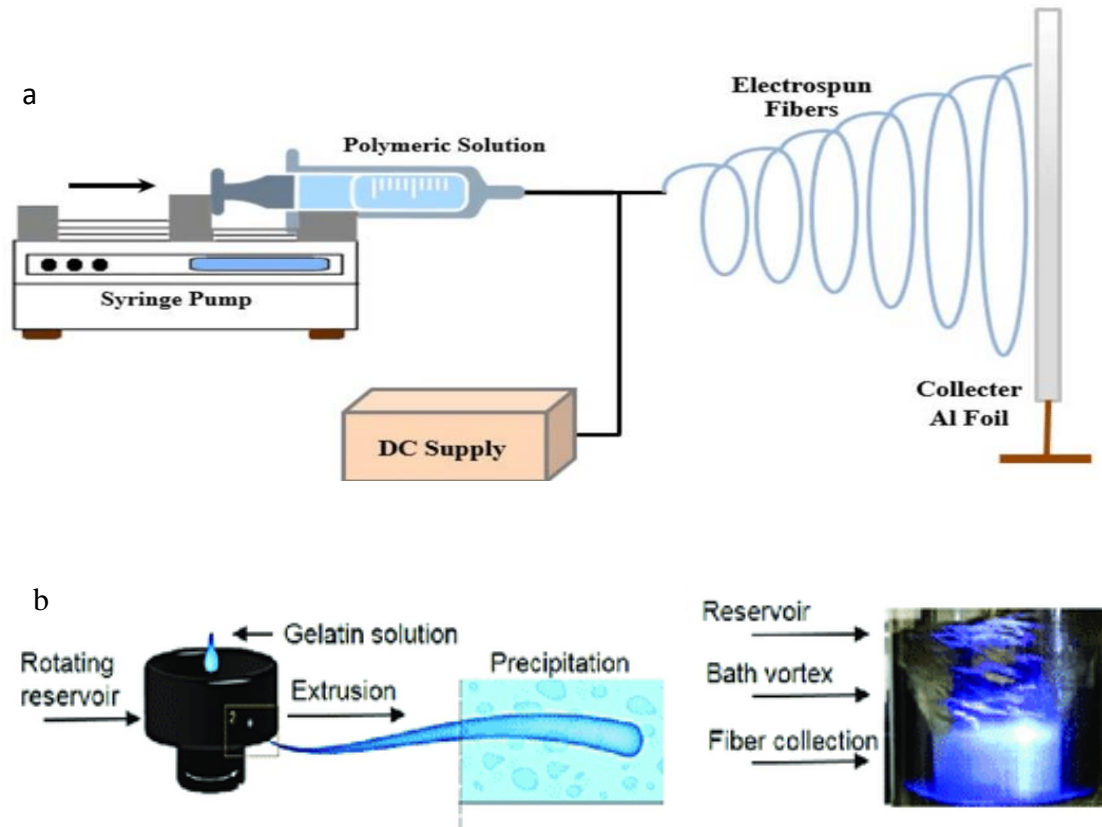


Figure 2.2. (a) Visual schematic of fundamental electrospinning concept⁴⁴ and (b) visual schematic of immersion rotary jet spinning concept⁴³.

Decellularized and Grown

Another method studied in tissue engineering, especially in the development of animal contribution reduced methods is decellularization of biomatter or the controlled growth of biomaterial to later be seeded with the desired cells. The decellularized method has been incorporated in medical practice as decellularized porcine aortic valves have been used in surgical replacement of defective valves in human patients with

proportionally low rejection from patients⁴⁵. The materials are decellularized using pre-defined chemical processes specific to the tissue being flushed of its cells⁴⁶. In addition, plant-based materials have been decellularized to leave the extracellular matrix to be seeded by the animal tissue cells. One of the decellularization methods that has seen significant interest is the use of spinach, an easily and quickly produced material, and is being highly investigated in the cultivated protein industry⁴⁷.

Similar to decellularization, methods have been developed in which a material that is easy to control in its final composition is used to fabricate scaffolds. One of the most promising methods of this is scaffold production is through solid state fermentation of mycelium or mushroom to form a foam scaffold in which the porosity of the material can be adjusted in various regions and is large enough to allow for cells to diffuse within the scaffold⁴⁸.

2.3 Commercial Equipment for Bioprinting

There are several commercially available systems for bioprinting applications. The bioprinting market is saturated with syringe extrusion-based methods which either incorporate pneumatic or displacement driven material extrusion controls. Below are some of the notable systems on the market currently.

2.3.1 Bioprinter 1 – Allevi 2

The Allevi 2, an extrusion-based desktop bioprinter seen in [Figure 2.3a](#), is controlled through a pneumatic system. Its operating system is all online in which the user downloads the files they wish to print and each of the printer parameters are defined

before each print by the user. This allows for significant control by the user on the printing cycle as needed for any material that is desired to be tested. The Allevi 2 can print from two syringes of varying materials if desired, has one heated tip, and a UV light for photocrosslinking the materials if required. You can print into multiple commonly used dishes and culture plates in cell-culture which reduces the likelihood that the printed construct will incur damage if transferred into the culture plate or petri dish post-print. A key disadvantage is the small size constraints as well as the potential requirement for printed support material to ensure the desired structures can be printed. This requirement for scaffold post processing on soft hydrogels is not feasible, which significantly reduces the part complexity possible in the extrusion-based method. The build area possible by the Allevi 2 is $9\text{ cm} \times 6\text{ cm} \times 13\text{ cm}$ ⁴⁹.

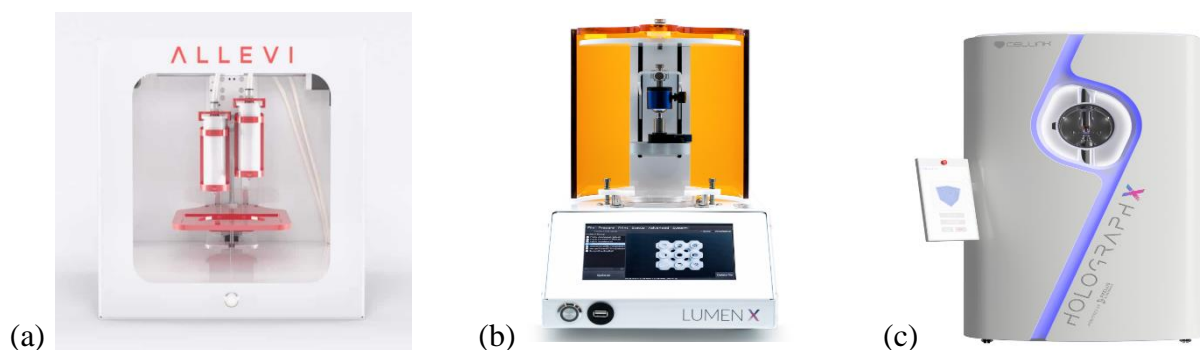


Figure 2.3 (a) Allevi 2 printer by Allevi⁴⁹, (b) LumenX SLA printer by CellInk⁵⁰, (c) HolographX holographic volumetric printer by CellInk⁵¹.

2.3.2 Bioprinter 2 – Lumen X

The Lumen X by CellInk, seen in [Figure 2.3b](#), is a stereolithography-based printer in which a resin bath is used and a projected light in a defined geometry based on the desired print structure is exposed to one layer of the material. A vertical collector

plate motion allows for the adjustment to the next layer to be printed. The final structure can be printed without the requirement of printed supports. This method can achieve high resolutions and does not experience variations from the printing stresses experienced from the extrusion process. The most significant drawback in this system is the amount of material required for one print. The build dimensions of the Lumen X are 6.5cm x 3.5cm x 5.0cm and has a defined pixel resolution of 50 microns with a z resolution of 5 microns. Although it has a good resolution, the build size is quite small, which limits the user's ability to mass-produce or scale up any printed pieces⁵⁰.

2.3.3 Bioprinter 3 – Holograph X

The Holograph X, also a product from CellInk as seen in [Figure 2.3c](#), is marketed as an extremely high-resolution printer that utilizes holographic projection to print true-to-form 3d structures. Although specific specifications are not listed, CellInk claims the Holograph X has the capability of printing microfluidic channels as small as 10 microns in diameter. The most significant disadvantage to this system is its print bed dimensions. The xy-plane is 12.5 cm × 12.5 cm with a z depth up to 0.27 cm at the high-resolution setup and up to 1 cm with a lower resolution. Although this technology does not require a layer by layer approach like the other two systems, it does not show promise for the mass production of larger scale tissue constructs unless reoptimized for that specific purpose⁵¹.

CHAPTER 3: BUILDING DRUM AND INITIAL TESTING

3.1 Motivation

As has been previously represented, a distinct lack of textural control and variation is heavily present in terms of tissue engineering. This is especially true for edible applications, of which we would be perhaps the most sensitive of this issue. One long-term goal of this field is to improve the speed of textured alternative protein production through the use of advanced edible biomaterials and innovative biomanufacturing tools. In addition, the improvement of the 3-dimensional control of the geometries therein is highly desired and would allow for significant optimization for the cellular atmosphere. In pursuit of this goal, one hypothesized method for accomplishing this is to combine methodologies, like photolithography to rapidly produce cell-laden constructs with biomimetic architectures reinforced by edible nanofibrous architectures. As such, this is determined to be the guiding goal for this research endeavor: testing photolithography as a method for increasing the rate of production of higher order cell-culturing constructs and characterizing the effects of adjustments in the scaffold architecture. In pursuit of this goal, the first objective is to develop a printing chamber that will allow for these desired structures and structural variations to be printed. The design considerations will be defined in further detail, followed by a description of the design and testing plans. The results of the preliminary tests will then be discussed as well as the future work required to develop this technology further.

3.2 Design Requirements

Before beginning the brainstorming and design phase, a list of design requirements must first be defined for the effectiveness in terms of tissue engineering applications. These requirements can be split into three categories: cell-culture compatibility, print quality of, and adjustability of material properties of the final printed sample. These are described in the following subsections and are used to determine the effectiveness of each design iteration and help to inform a decision on the best methodology for the printing or scaffold fabrication process. These requirements will help to guide the initial design iterations to further identify what components effectively accomplish the desired goals in the final design.

3.2.1 Cell-Culture Compatibility

One of the key considerations for the effectiveness of the developed design is the innate compatibility with cell-culturing technique requirements. In order for this design to be fully utilized, the equipment must be able to fit into a biosafety cabinet, which are most commonly two configured sizes of 4' and 6' models. To ensure full compatibility, a 4' model will be used to define maximum possible dimensions. With common maximum inner dimensions of the 4' cabinet at 47" by 26" by 26", as defined by the Biotect Elite 4' Class II model (Global Lab Supply, Orange, CA). In addition to having a restriction on size, the equipment must also be easily sterilized through ultraviolet exposure, autoclave, or chemical sterilization. This typically requires the material to withstand the chemical exposure or autoclaving heat and pressure as well as geometrical considerations to ensure no areas will be impossible to sterilize or collect any chemicals that could cause harm to

the cells or the photolithography process. Finally, none of the components in contact with the scaffolding material shall have a known toxicity to cells. These ideas can be more concisely defined in the following subsections.

3.2.2 Print Quality

In addition to being cell-culture compatible, the printer must provide a few key advantages in the final build achievable through the fabrication process. A high resolution of print can have a significant effect, both on part accuracy with the intended print and effectiveness of use for cell culture. As described previously, in order to create thick cell-laden constructs, vascular paths must be present within the scaffold to ensure nutrient supply and waste removal of the cells within the construct. With a higher resolution, these vascular paths are more easily and effectively constructed, with the potential of creating more biomimetically sized pathways, which venules can range from 8-100 micrometers. The target resolution for this project is 10 to 20 microns. This high resolution desired must also be balanced with the speed at which the print can be completed. Especially during cell-laden printing, it is crucial for the print cycle time to be minimized to reduce cell necrosis within the material. The optimal time for print was determined to be less than one hour for a 2.54-centimeter-thick print, or 2.54 centimeter thickness per hour. Finally, the ability to adjust the orientation of layers allows for further control of the part as well as its final bulk mechanical properties under stress.

3.2.3 Adjustable Material Properties

To achieve the highest effectiveness for research purposes, the ability to adjust the material composition and handling significantly increases the testability of varying hypotheses for successfully controlling the mechanical properties of the scaffolds created. This tunability includes the concentrations of the components of the base hydrogel material as well as the processing of the base material. This processing is determined by the printing parameters such as wavelength of the light used, exposure time, and layer orientation. As the material can be controlled separately from the printing system itself, the requirements of the system design will be defined as the ease of adjustment per printing requirement and includes the light source as well as the controlling system. A tunable wavelength that can be used to cure between the range of 385 and 405 nanometers is in the near visible ultraviolet range which has been proven to both successfully radicalize certain photoinitiators while maintaining cell survivability at a high level. The light intensity should also be adjustable to manage the amount of photons entering the material at a given rate, as well as an adjustable exposure time for the same purpose. Finally, a user friendly control interface would be highly desired. For the optimal application, these systems should require minimal training and maintenance and be nearing an automatic system. This reduces the load on the workforce it brings forth and the potential for pitfalls.

3.3 Design Process

With the aforementioned criteria in mind, three designs were evaluated: An upward motion collector plate, a flooded laid fiber network, and rotational volumetric printing. Though each will be discussed in further detail, the key feature of design 1 is the

simplicity of translation from a desired print to the print process in coding, mimicking traditional photolithographic methods. The key feature for design 2 is the one-layer cure methodology that reduces mechanism complexity. The key feature for design 3 is the complex structuring with no layering approach. Upon defining the systems, the criteria will then be applied to them and utilized to determine the best method.

3.3.1 Design Option 1: Upward-Motion Collector Plate (UMCP)

The initial proposed design, seen in [Figure 3.1](#), imitated a traditional photolithography system in which the pre-hydrogel resin is held within a resin bed. A flat collector plate is attached to a vertically oriented linear actuator and positioned above the resin bed. A mirror is placed under the resin bed to reflect the image projected from a projector or optical engine placed in front of the resin bed. At the start of the print, the collector plate is lowered into the resin bath where the plate is one print layer height apart from the bottom of the resin bath. The print parameters can be controlled through a coded system that includes control of the projector and the linear actuator.

Advantages

This system is advantageous as it is the simplest and most understood method due to its direct correlation to current photolithographic systems. The two-dimensional layer by layer stacked approach allows for simple programming to convert the desired print into a coded cycle which reduces the amount of time required to optimize the print settings. This method can also be adjusted to use a photo mask attached to the bottom of

the resin bed. In this way, the programming is further reduced to only require on-off commands for the light projector.

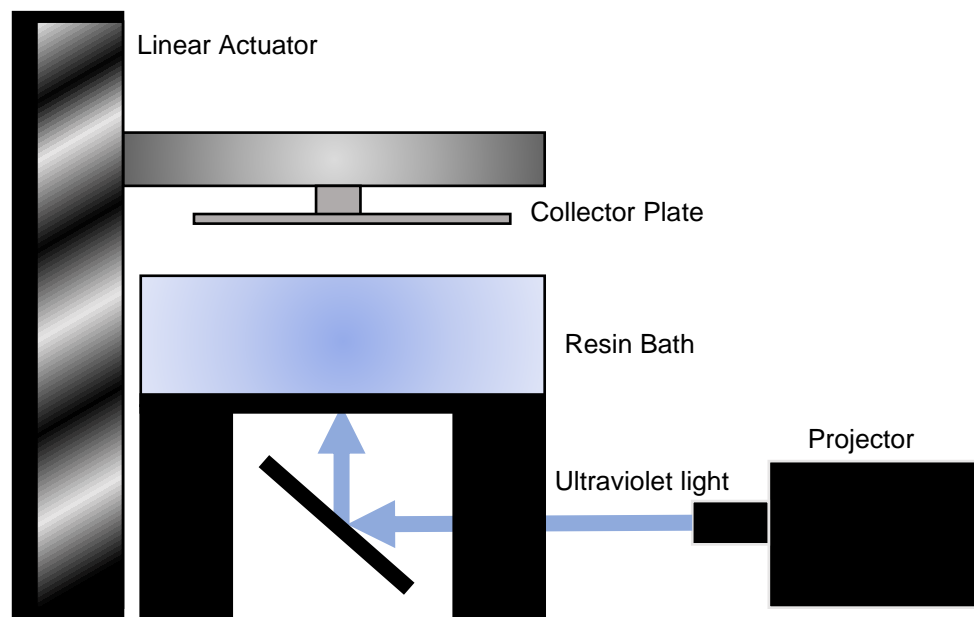


Figure 3.1. Proposed schematic of design iteration 1, the upward motion collector plate system.

Disadvantages

Going hand-in-hand with its increased simplicity in design and set-up, this method allows for the least amount of control and variation in the print volume. If a photo mask is used, this either requires frequent changes of the photo mask or to have a final product that is based solely on a two-dimensional design that is extruded into a three-dimensional shape. This significantly limits the amount of control of the vasculature placement. If the print geometry is defined by a projected pattern, the resolution of the printed layer will be based on the projection source as well as the distance the light must travel before curing the material. Finally, if an intermittent

scaffolding material is to be inlaid, such as electrospun fiber sheets, it will be a tedious process which either requires an additional control system to be run during the print or for the print process to be paused and the intermittent layer to be inlaid by hand before proceeding with the print. This can be a messy and inconsistent process and lead to poor print resolution and significant differences between the expected and realized parts.

3.3.2 Design Option 2: Flooded Laid Fiber Network (FLF)

The second design, as seen in [Figure 3.2](#), focused on the need to control the intermittent layer orientation rather than the layer by layer curing of the hydrogel. In this system, the print bed is the same as the previous design, but there is no incorporated linear actuator. The fiber layers are oriented between two plates and secured. The volume of the print bed is then flooded with pre-hydrogel material. After the material has been flooded through the fibrous layers, the bed is then exposed to projected light, similar to the previous method. Instead of a layer by layer curing approach, the bed is subjected to photocuring for an extended time period. Through this extended exposure time, the photocrosslinking will initiate at the base of the bed where the first contact with light occurs and will then continue to crosslink upward as the light perfuses through the material.

Advantages

This method allows for the most control over the orientation of an intermittent scaffolding material within the final build as the layers are placed in their desired orientations and the pre-hydrogel material is added around the fibers. The design is once

more very simple on the controls side as after the fibers are laid, the only control is determining the light intensity and exposure time of the projected light. Since the intermittent material is already placed, there will be little to no delay between the print layers that is required in the previous design. Finally, without moving parts, there is less potential for error to occur during the fabrication process.

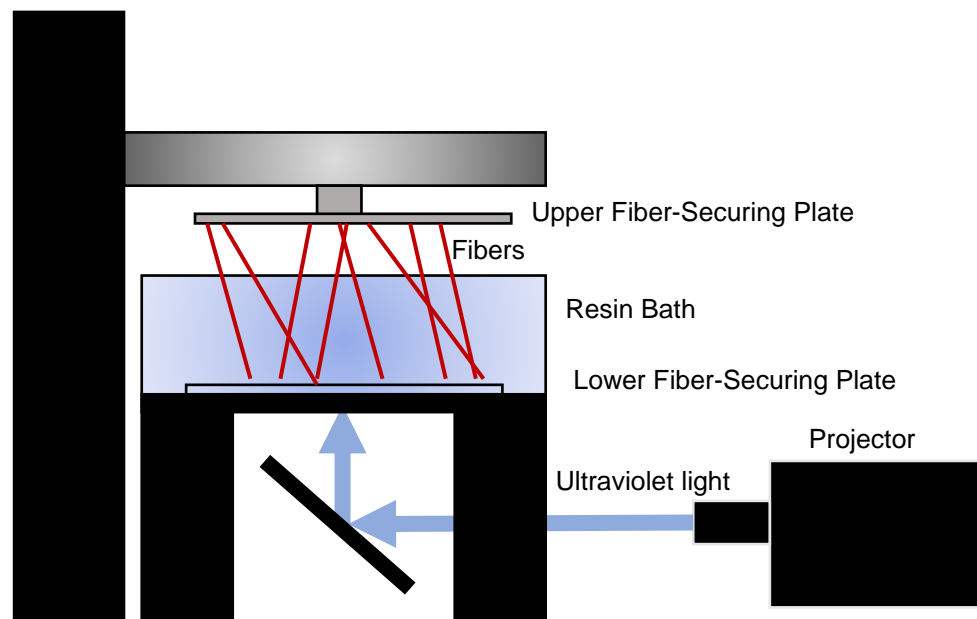


Figure 3.2. Proposed schematic of design iteration 2, the flooded laid fiber network system.

Disadvantages

This process, unless an automated fiber orientation system is created, would require significant preparation time before the print. The fabrication and exposure method could potentially be altered to incorporate layer by layer curing, but would require significant design considerations, such as a method for ensuring the anticipated layer height is achieved when flooded with additional pre-hydrogel material as well as the

direction of light exposure to successfully cure the new layer of material. If layer by layer adjustments are not made, the maximum thickness printable through this method is significantly reduced due to light perfusion through the material. The hydrogel may also crosslink inconsistently throughout the material, or have a gradient of crosslinking intensity, which reduces the control of the bulk material properties. Other than this method for creating anisotropy within the material, the layer by layer adjustment in curing parameters cannot be achieved through this method.

3.3.3 Design Option 3: Rotational Volumetric Printing (RVP)

The third design investigated, as depicted in [Figure 3.3](#), is a photolithographic printer that utilizes a volumetric approach to curing the hydrogels in space. In this system, the resin bed from the previous designs has been replaced by a rotating resin chamber. The light projector is aimed directly into the chamber and set to specific projections to cure the hydrogels in specific regions within the volume of the pre-hydrogel material, based on the material properties as well as the speed of rotation of the chamber and the light projection settings and image pattern.

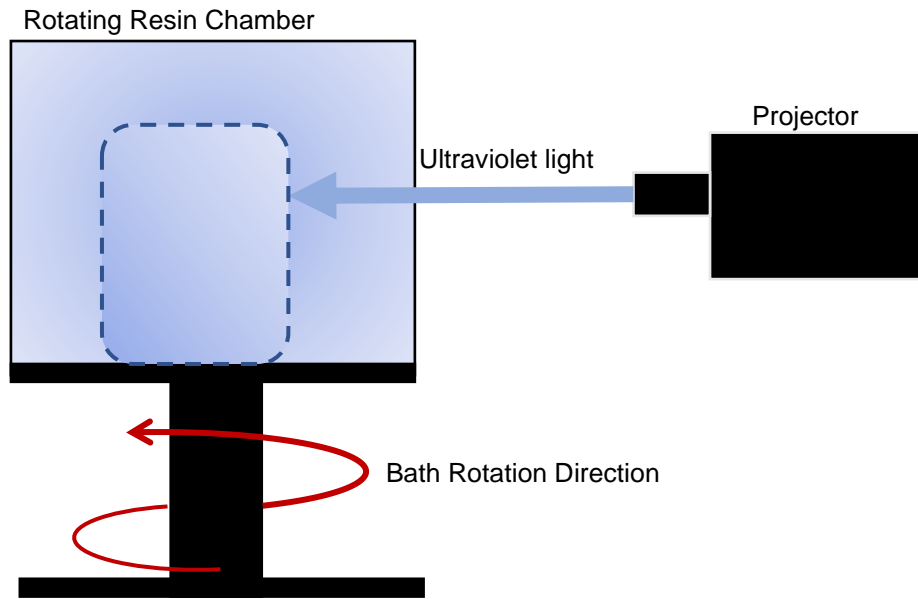


Figure 3.3. Proposed schematic of design iteration 2, the rotational volumetric printing system.

Advantages

The volumetric curing method has been studied recently by other academic research groups and has proven to be a viable method for speeding up the printing process for photolithographically constructed objects. Due to this research thrust, some open source designs and software have been made available through the corresponding researching groups. In addition to the speed, this method has been shown to effectively and safely cure cell-laden hydrogels. Finally, the volumetric curing method could allow for an increased complexity and may provide an additional platform for pre-defined scaffold orientation that is then flooded by the pre-hydrogel material and then cured. In addition, this method removes the requirement for supportive material to be printed as it cures within the material.

Disadvantages

One of the biggest disadvantages of this method is its complexity. Though materials are open sourced, if any variation is made the system needs to be recalibrated from the ground up. Upon consultation of some of the open source software⁵², there are dozens of variables that must be incorporated, such as viscosity and refractive index of the material, photoinitiator type and concentration, and so many more. It also would be quite difficult to incorporate a secondary material such as nanofibers for structure as these fibers would block the light from diffusing within the volume as desired. Though it offers a very futuristic replicator feel, significant hurdles stand in the way of this being a truly show-stopping method, especially for large-scale manufacturing.

3.4 Evaluation of Methods

In order to quantify the design iterations and their effectiveness the criteria for determining best methods were defined. Each iteration was then analyzed against the defined criteria through weighted Pugh matrices. The evaluation criteria as well as the corresponding Pugh matrices are detailed further in the following subsections. The results of the Pugh matrix analysis can then be used to determine an optimal final design.

3.4.1 Evaluation Criteria

Evaluation criteria were defined to create a metric for quantifying the most beneficial design method. Using the Pugh matrix methodology, one design is defined as the control design in which each alternative design is directly compared. If the alternative design is better with respect to the specific criterion, it receives a 1 rating, and if it is

neutral or negative it will receive a 0 or -1, respectively. These criteria were then weighted on importance, ranging from 1 to 5, where 5 signifies the highest importance. A total sum from all weighted criteria is then calculated to determine if the control is better than the alternative methods, or when the alternative scores are all negative. For each criterion, a description of its meaning and its corresponding weight factor is described as follows:

Adjustability of Layer Orientation

This criterion refers to the ability to manipulate the orientation of the intermittent material layers within a three-dimensional space. The weighting assigned to layer orientation adjustability of 5 was one of the two highest as it allows for the most experimental analysis on the control of anisotropy. For example, if you are able to control a two-dimensional slice architecture you are only able to adjust the properties on that defined plane. If you are able to treat the adjusted layer as a 3-dimensional surface with varying complexity, you can still define your layer as a two-dimensional plane with a constant third dimension, or you can create more complex surfaces.

Adjustability of Material Properties

Adjustable material properties is in reference to the material properties achievable within the fabricated scaffold throughout the final build. This could include material concentration adjustments as well as print variations that can have an effect on the crosslinking severity, which in turn adjusts the mechanical properties in that region of the print. This was also rated with the highest weighting of 5 as it is a secondary method for

controlling the anisotropy of the build which is the desired overall functionality this printer is to accomplish.

Setup Time

Setup time includes any routine steps for preparing the equipment for a print, such as the time required to refill or properly place any of the materials required for each print. This metric received a mid-range rating of 3 as it does not hinder the ability to create the desired part. It does, on the other hand, play a large role in the ability for the design to be scaled up and utilized in future industrial applications.

Manufacturing Cost

The manufacturing cost is the cost of materials and time required in manufacturing the equipment itself. As the materials used in the pre-hydrogel material is highly user dependent and requires additional research to determine the best material aligned for each individuals needs, the most direct comparison available for the cost of the system is through the analysis of the cost to build the equipment. This was weighted as a medium-low priority at 2 as once the equipment is fabricated, there will be a life to the equipment in which the price of the equipment itself can be dispersed as a cost factor for each build produced from the equipment itself. This life can be highly dependent on additional factors such as frequency of use, quality of equipment components, and maintenance practices for the system.

Optimization Simplicity

A big factor in the use and development of a system is the time and materials required to optimize the system to achieve a final product desired. Similar to the natural ability to adjust the material and layer orientations, this more pertains to repeatability and the complexity required to turn over to create a different internal architecture or print cycle. Especially during research and development phases, a simpler and speedier turnover to be able to make adjustments increases the overall output capable of the system itself.

User Input Requirement

User input requirement defines the amount of manual or intellectual input required to complete any of the needed tasks during the operation of the equipment. For example, if the user must change over or prepare additional components of the machine or prepare the materials in any tedious manner, this would increase the manual input. Adjusting the coding per run, on the other hand, would significantly increase intellectual input. This is an important consideration as it would reflect the complexity and manpower required to run the system in a scaled up industrial setting.

Coding and Conceptual Simplicity

This metric is heavily based on the development process of the system. As the conceptual complexity increases, this will waterfall into multiple areas of the process. For example, with the rotational volumetric printing, the added motion of the bath may induce fluid motion within the materials which could hinder crosslinking and decrease

the resolution of the print dependent on the smoothness of the motor motion controlling the rotation. In addition, if there are many moving parts that all need to be controlled simultaneously, this can increase the sources for failures and bog down the computing system.

Maintenance Simplicity

Maintenance simplicity defines the overall maintenance of the system itself. This can include preparation, such as sterilization, as well as the clean-up process or any routine care that the machine may need. In addition, an increased system complexity can require significant time spent conducting calibration and functionality testing on the individual components. Ultimately, this metric serves as a consideration for the foreseen maintenance requirements when used in future industrial applications.

3.4.2 Weight Factors

The adjustability of the layer orientation and adjustability of material properties were weighted at the highest level of 5 as they are the key criteria that allow for full investigation of the fabricated structures and the effect that each structure adjustment has on the bulk properties. The next highest weighted criterion at 4 is the user input requirement. This signifies how automated this process can run, which is crucial to industrial applications of mass production. Setup, optimization, and maintenance are weighted at 3 as they once more identify how easily the equipment can be utilized both in research and development as well as in industrial settings, identifying the cost of the equipment while not in full production. Manufacturing costs follows at a level of 2, as

this type of equipment should have a long life and be financed as an initial business equipment investment. Finally, coding and conceptual simplicity was weighted at a level of 1, as it does have a significance in the initial development of the system, it should be compensated for in the created user interface.

3.4.3 Pugh Matrix Results

As alluded to previously, the above defined criteria for comparison were used to evaluate the design iterations in question for the system setup. The first system that was used as the control system was the flooded laid fiber network (FLF,) and the results from this initial Pugh analysis can be seen in [Table 3.1](#). After tabulating the results, it was determined that both of the alternative methods would outperform the control. The most significant drawbacks of the flooded laid fiber network is the low adjustability of the material properties and a high requirement of user input. It's conceptual simplicity, on the other hand, is an advantage that significantly decreases the efforts required to develop and optimize the system.

Table 3.1 Pugh matrix iteration 1 with flooded laid fiber network (FLF) as the control

Criteria	Weight factor	FLF (Control)	UMCP	RVP
Adjustability of Layer Orientation	5	0	-1	0
Adjustability of Material Properties	5	0	1	1
Setup time	3	0	1	0
Manufacturing Cost	2	0	1	0
Optimization Simplicity	3	0	1	0
User input requirement	4	0	1	1
Coding/ conceptual simplicity	1	0	-1	-1
Maintenance simplicity	3	0	0	-1
Total Scores		0	11	5

Table 3.2 Pugh matrix iteration 2 with upward motion collector plate (UMCP) as the control

Criteria	Weight factor	FLF (Control)	UMCP	RVP
Adjustability of Layer Orientation	5	0	1	1
Adjustability of Material Properties	5	0	-1	0
Setup time	3	0	-1	0
Manufacturing Cost	2	0	-1	-1
Optimization Simplicity	3	0	-1	0
User input requirement	4	0	-1	0
Coding/ conceptual simplicity	1	0	1	-1
Maintenance simplicity	3	0	0	0
Total Scores		0	-11	2

Based on the nominal valuation of the alternative methods from the first analysis, the Upward Motion Collector Plate was set as the control system, as documented in **Table 3.2**. The flooded laid fiber network still was unfavorable in this analysis, but the comparison between the UMCP control and the rotational volumetric printing system was further investigated. A key advantage held by the rotational volumetric printer over the control is the adjustability of the layer orientation, one of the highest weighted criterion. The drawbacks that rotational volumetric printing, on the other hand, is the cost of manufacturing as it has a significantly higher requirement for light projector quality and additional system components as well as an increase in conceptual complexity to take a desired print and create the projection print cycling required to cure the part properly. Although the control was better than the flooded laid fiber network, the rotational volumetric printer was rated slightly higher than the control system.

Table 3.3 was created to more intuitively summarize the previous findings that the rotational volumetric printer, set as the control, was quantified as a better method for the defined purposes and criteria. Although the rotational volumetric printing undeniably

outweighs the flooded laid fiber network, the upward motion collector plate method was only slightly underperforming than the volumetric printing method. This will be an important factor considered when finalizing the printer design, as will be described in the following section.

Table 3.3 Pugh matrix iteration 3 with rotational volumetric printing (RVP) as the control

Criteria	Weight factor	FLF (Control)	UMCP	RVP
Adjustability of Layer Orientation	5	0	0	-1
Adjustability of Material Properties	5	0	-1	0
Setup time	3	0	0	0
Manufacturing Cost	2	0	0	1
Optimization Simplicity	3	0	0	0
User input requirement	4	0	-1	0
Coding/ conceptual simplicity	1	0	1	1
Maintenance simplicity	3	0	1	0
Total Scores		0	-5	-2

3.5 Final Design: Digital Rotational Ultraviolet Manufacturing (DRUM)

After completing the Pugh analysis, the rotational volumetric printing system was narrowly defined as the optimal method with the upward motion collector plate at a close second. In order to ensure the final design was objectively the optimal solution, a combination of these two methods was constructed, aiming to utilize the benefits of each system while reducing the drawbacks. This new design, identified by its acronym DRUM (Direct Rotational Ultraviolet Manufacturing,) can be seen in [Figure 3.4a](#). This new design was then taken from the conceptual state into an initial prototype, seen in [Figure 3.4c](#), to be tested for functionality.

The novel DRUM printer is similar to a traditional upward motion collector plate method of digital light processing in which the overall layout includes a stationary resin vat, a collector plate, a projector for light production, and a linear actuator for z-axis motion. In addition to the traditional collector plate system, modifications to the collection motion were introduced. Instead of the traditional flat collector plate, a novel collection system was designed in which a rotating collecting shaft is used to induce motion during the printing process. In general, this allows for additional control to the three-dimensional architecture of the printed part. The manufacturing process for this system and its components will be defined in further detail in the subsequent manufacturing section of this report.

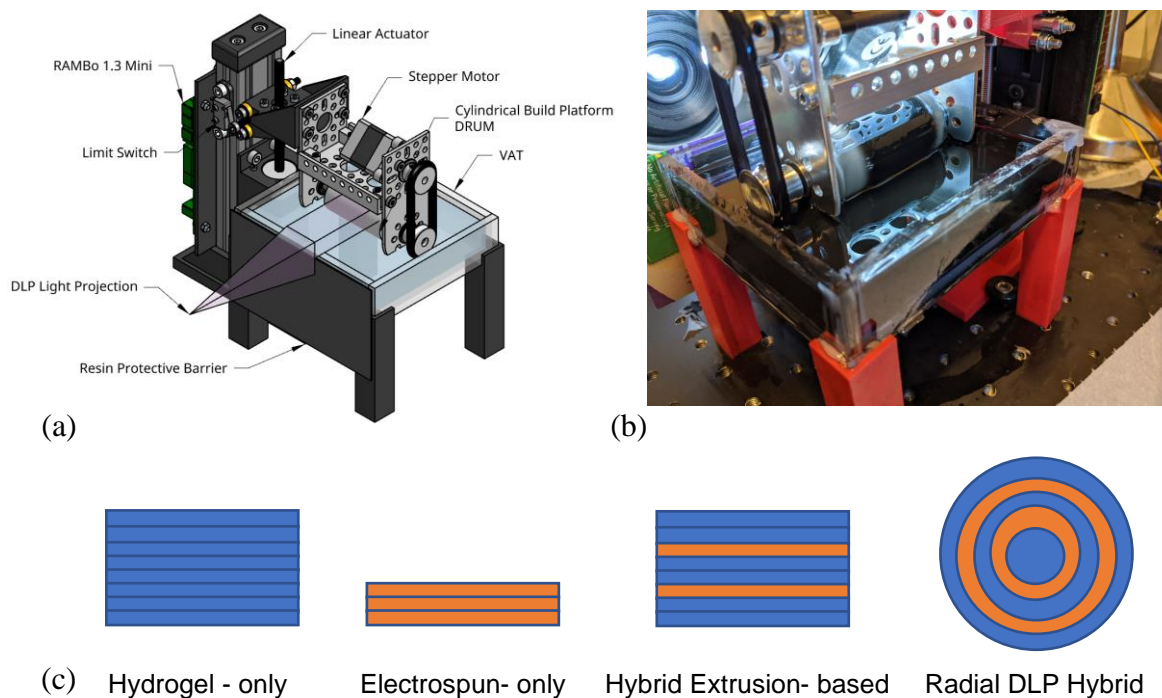


Figure 3.4 (a) CAD model of Digital Rotational Ultraviolet Manufacturing (DRUM). (b) Image of the DRUM printer during operation. (c) Layer cross-sections for hydrogel (blue) and electrospun fiber sheets (orange) for layer-by-layer and radial-layer prints.

3.5.1 Key Features

The final printing system design can be further broken into eight key features.

These features are identified in the following list:

- **Modular rotational/flat collector plate system:** Utilizing a modular or replaceable collector plate system allows for multiple printing pattern designs to be tested. In this particular case, the upward motion collector plate system with a flat plate that moves only in the z-direction through the actuation of the linear actuator can still be tested to reference. As this is a modular component, additional iterations can be easily fabricated and tested in this assembly.
- **High resolution linear actuator for z-control:** This high-resolution linear actuator, set at 1mm per revolution which easily allows for a 10 μm layer height capability, defines the resolution in the z-direction of the print, where the higher the resolution the smaller the layer thickness. This factor is most directly utilized in the flat collector plate setup and plays a role in the overall print resolution of the final print.
- **High resolution light projector:** Using a high-resolution light projector further increases the resolution in the xy-plane of the print. The resolution of the projector used in the initial prototype of the system has a resolution of $1920 \times 1080\text{p}$. The actual projector used was the modified projector supplied with the commercially available B9 Creator SLA system (B9Creator, B9Creations, Rapid City, SD) with a pre-defined print resolution of 30 to 70 μm . In future studies, this projector will be replaced by a custom optical engine (Wintech

PRO6500-405nm, Wintech Digital, San Marcos, CA) for further improved print performance and adjustment.

- **Three-dimensional layer-by-layer curing pattern:** In the rotational collection setup, the nature of the collection system allows for layers to be cured and collected radially and continuously. This capability allows for distinct layer changes in curing patterns to be defined in a three dimensional space. In addition, as it is continuous curing, the crosslinking pattern for the material will naturally follow the rotational pattern of the print.
- **Adjustable collector plate rotational speed:** Having the ability to adjust the rotational speed of the rotational collector shaft is important in print quality control. As the rotation induces fluid motion within the uncured resin, the adjustment of the rotational speed will directly affect the radial layer thickness.
- **Intermittent layer feeding (optional):** In addition to adjustments made on the treatment of the hydrogel curing layer by layer, this system also allows for the incorporation of an additional system component: a fiber mat or rolled material that can then be directly fed into the print cycle, creating a more reel-to-reel manufacturing process.
- **Acrylic resin bed:** The resin bed was created from cell-culture safe, clear acrylic sheets. This component is important as you need to ensure the projected light is able to travel through the resin bed barriers to cure the resin in the desired location.
- **3D printed structural components:** These structural components, such as the brackets that hold the collection system to the linear actuator and the legs that

keep the resin bed at the optimal height for printing, can be easily tailored dependent on the new needs that may arise for the system.

3.5.2 Advantages

There are several key advantages that make this system modified from previous designs an optimal configuration for research and development purposes. At the same time, there are inherent disadvantages or hurdles that will need to be addressed about this design to further improve its functionality. A strong understanding of both is required to fully investigate the quality of the final design proposed. The advantages of the system can be broken into the following:

Adjustable Material for Printing

One of the most significant advantages to this DRUM system is its inherent capability to adjust the materials properties of the printed sample. This can be broken down into two key adjustment types: (a) through the variation of printing parameters per layer and (b) through adjustments of the material itself.

Much like adjusting the projected light patterning per layer to change the geometry of material crosslinked, the light intensity and exposure time can also be adjusted per layer. With a material such as GelMA which will be studied using this system, the crosslinking severity has a significant impact on the bulk mechanical properties. Using this manipulability, an anisotropic bulk mechanical behavior can be printed using the same material merely with layer treatment adjustments. Investigating the effect that radial cured layers utilizing this method could improve the

manufacturability of failure characteristics of these scaffolds to achieve a more skeletal muscle tissue mimetic behavior.

There are two foreseen sub-methods for adjusting the materials present within the system. The first method is to wrap intermittent layers of prefabricated structural materials, such as electrospun fiber mats, within the hydrogel to add a composite structural integrity and natural fault lines during material failure under loads, as depicted in [Figure 3.4c](#). The second method for material adjustment is to adjust the hydrogel itself. In adjusting the material composition, such as increasing the photo-initiator concentration or adding a photo-absorber to increase or decrease cross linking efficacy respectively, you are able to achieve similar adjustments in mechanical properties from layer to layer as achieved through the adjustment of light intensity or exposure time as previously described. In order to accomplish this multi-material system, the simple resin bed present in the base system would need to be improved upon to include multiple resin beds available throughout the printing process.

Increased Rate of Volume Cured Per Time Interval

When determining scalability and usefulness in high rate industrial production, the speed at which the product can be fabricated is a crucial metric. With this continuous curing system in which there is no time required to adjust the collector plate to reset the layer height for the new cured layer, this significantly decreases the time required for a single print. This is also considerably more efficient than an extrusion-based method for construction, as the material can be cured in layer scanning rather than patterns limited by the extrusion nozzle diameter and flow rate. Especially when considering this equipment

for the use in constructing meat alternative protein structures, the level of production could be a significant hurdle in adopting various technologies, and addressing the speed issue can help to validate the methodology.

Shape and Orientation Adjustment

When constructing parts, especially when variations are desired within the final build, the ability to adjust the overall shape and orientation of its components holds a heavy weight in creating these parts successfully. With the proposed system, the modular design to create layer by layer parts in which the layers are either flat and parallel to each other or concentric by nature of the collection process is a big step in the direction of more simply adjusting the orientation and shape of the resulting part, seen in [Figure 3.4c](#). In addition to the layer orientation itself, using a digital light processing method, it is possible to further manipulate the geometry of the part based on your projected light patterns or curing process, as discussed previously.

Relative Simplicity to Alternative Methods (RVP)

Finally, a significant advantage that this proposed method holds, especially over the rotational volumetric printing, is its improved conceptual simplicity. Although the rotation of the collector plate adds forces within the system that must be accounted for, this can mainly be accounted for through optimization of the print parameters such as the collector plate rotation, or the material viscosity. When considering the rotational volumetric printing method, the material is intended to be cured within the bulk material. This decreases the margin for error in the system and requires significant testing and

verification of the printing parameters to ensure that no material is cured that is not intended. The reduced complexity in developing the control system significantly reduces the time required to optimize the system itself and simultaneously reduces the complexity when translating this currently research-only technology into a full-scale industrial equipment as it reduces the high level knowledge base required to conduct the optimization process.

3.5.3 Disadvantages

The disadvantages to this system all currently stand as aspects capable of being addressed directly to ensure the system functions at full capacity. These disadvantages are as follows:

Effect of Fluid Dynamics

As alluded to previously, the addition of a rotational motion component further adds complexity to the system. This rotation induces fluid motion within the system, causing the fluid dynamics, most specifically the boundary layer conditions and their effect on the layer thickness, is crucial to understanding the mechanics and optimization of the system. In addition to flow induced boundary layer effects, effect the rotational speed has on the layer height and consistency is compounded as the effects of gravity on the uncured resin settles from the surface of the collector plate. This, again, can be addressed through optimization for each material and the atmospheric conditions, but if left unaddressed could lead to significant deviation from the expected print and even total print failure.

Size Constraint

In its current configuration, the build area is quite small due to the limited requirement of sample sizes for experimental studies. This system would require scaling up for the production of actual meat cut products as the build area currently possible would only be 10 cm by 10 cm maximum with a maximum height of 2.54 cm. This sizing consideration can also be felt through the limitations of having an internal core for the rotational collection system. A developed coreless method for the production of these hydrogel scaffolds would significantly improve upon the manufacturing model itself.

Lack of Full Printing Analysis

At the time of preparation of this report, the full capabilities of the printing process have not yet been tested. This will be identified further in the testing section to follow. Although promising, the effects that the fluid motion from DRUM rotation has on the print integrity has yet to be quantified. There is still much to be developed and tested to better understand the full advantages and limitations that the manufacturing method proposed possesses.

3.6 Manufacturing

This section will discuss the manufacturing of the proposed printer itself and any additional modifications suggested to improve upon the system.

3.6.1 Materials

The materials used in the fabrication of the printer, as defined in the design requirements, needed to comply with requirements for cell culture study safety. They needed to be fabricated of non-toxic materials that were easy to clean using at least one of the accepted sterilization methods recognized in the field of biology and cell culture.

Table 3.4 serves as a comprehensive list of the materials in contact with the hydrogel or resin used in the final design of the printer prototype. As can be seen, all materials, after they have achieved their final designed structure, are non-toxic to cell culture. All other components of the system, aside from the bracket securing the collection system to the z-axis linear actuator which is also printed from PLA, are commercially available and capable of sterilization through traditional cell culture sterilization techniques. A full list of the components used in the fabrication of the printer can be found in the Appendix, **A1**.

Table 3.4 Components of the printer model in contact with the resin/hydrogel base and the corresponding materials

Component	Material(s)	Toxic?
Resin Bed	Clear Acrylic (.22"), Acrylic glue	N, Y(pre-cure, N post-cure)
Resin Bed Stand	PLA (extruded print)	N
Rotational collector shaft	HDPE	N
Flat collector plate	TMSPMA-Coated Glass	N
Rotational collector carriage	Stainless Steel	N (will not cause excessive necrosis)

3.6.2 Required Component Features

A majority of the equipment components was commercially purchased. The key features required of the performance-sensitive components can be broken down into three

subsystems: the projector and overall structural system, the collection plate system, and the resin bath system. Within each of these subcategories exist specific requirements to achieve the optimal print capabilities. As these are the guidelines for the construction of the prototype or academic system, the optimization of feature selection may require adjustment when an industrial scaling of the technology is of interest. All components referenced can be found in [Appendix A1](#).

Projection and Structural:

The projection and structural subsystem serves as the backbone of the DRUM system itself and heavily defines the achieved print resolution as well as the range of applications and locations that the equipment can be used in. The most crucial factor in determining the achieved print resolution is the quality and performance of the light projection system used. The first requirement to the projector is the ability to print in the ultraviolet light range between 385 and 405 nanometer wavelengths. This range is required to cure most commercially available resins and ensures the printer system will successfully fabricate a final part after a cure cycle. The second requirement of the light projection system is a high natural resolution. This is defined of the system as a pixel resolution of the projected light. The defined minimum resolution of this system was defined as 1920 x 1080 pixels, which has been proven to achieve resolutions of 10 μm ⁵³. The high projected image resolution directly correlates with the resolution of the print, which limits the size and complexity capability of the printer system itself.

The core structural setup of the system has a high level of variability but can once more significantly impact the applicability of the system. Since this system is desired to

be used in cell culture studies at present, the structural backbone of the system must follow the guidelines of cell-compatibility and ease of cleaning. This must also be firm in its construction as any loose components or oscillations can significantly reduce the print efficacy or the achieved resolution. The components must not be subject to rusting or contain large grooving that may make sterilization burdensome or ineffective, leading to a coated metal or hard chemical resistant plastic as ideal material candidates for the structural components.

Resin Bath

Similar to the core structural components, a general ease of sterilization and chemical resistance is necessary for this subassembly. As these components fall in direct contact with the scaffolding material and potentially cell laden materials, it is crucial that the cytotoxicity of the materials used is minimized. A clear acrylic was chosen for the main construction material of the resin bath, as identified in the bill of materials located in the Appendix. This clear acrylic is non-toxic and transparent, allowing for the projected light to pass through the resin bed to cure the resin onto the collection plate. The acrylic thickness of .22” also is an ideal sizing as it exhibits sufficient structural integrity while still maintaining clarity through the sheet. This sizing can also be used to construct the assembly by hand where thicker sheets may require more intensive tooling.

The main bath is adhered into a single component through acrylic glue, which gives a good hold and is directly compatible with the acrylic sheets. Other gluing methods may be at risk of chemical reaction with the pre-cured resin. Once the bath is assembled it is placed into a structural base. As defined previously, this base must be

easily sterilized, but it does not hold the same requirements for surface treatments or otherwise as the components directly in contact with the resin or hydrogel solutions. In the initial prototype of the system, these components were 3D printed using an extrusion-based polylactic acid filament. The structural components could alternatively be constructed of coated metal, molded plastic, or additional acrylic sheet material.

Collection Plate

Finally, the collection plate system can be broken down into the rotational controlling motor assembly and the collection plate itself. There are two potential defined orientations of the collector plate itself: a traditional flat plate rigidly attached to the linearly actuated carriage or the rotation inducing system that includes a rotating shaft as the collection surface. For the latter orientation, the motor assembly must exhibit smooth rotating functionality with minimized oscillation of the collector plate. In order to reduce unwanted movements, pulley system was created in which a thick rubber ring was stretched between two axles- one connected to the motor and one connected to the collector- which held the components taught and in position. This pulley system is housed on a stainless-steel metal frame that minimizes the effect of material wear and creep from the constant force being applied through the rubber ring.

Depending on the requirements of the printing material, the chosen material for construction of the collection plate can vary. With both traditional photopolymerizable resins and hydrogels intended for cell culture studies, the printing material must be capable of crosslinking onto the collection plate or shaft. With the resin, this requires choosing the collection body of the same or similar plastic, but will make removing the

part from the collection system difficult to nearly impossible. A coated material may also be used, such as a coated or surface treated metal, which will encourage crosslinking onto the surface but will not cause permanent bonds with the collection body. This is ideal for the system and its ability to be reused. Similar to the resin system, the most effective method for ensuring crosslinking onto the collection body is to incorporate a coating onto the collection body itself that has been formulated to specifically crosslink with the material. For the use of GelMA as the hydrogel, a coating such as TMSPPMA can be used to effectively crosslink the material to a surface such as a glass plate or slide. The choice in material composition of the collection plate and any surface treatments given to the plate has a significant impact on the efficacy of the printer to create one monolithic structure as intended.

3.6.3 Cost Analysis

As defined in Table A1-4, the total liberal cost of the DRUM system is \$10,355.08. With this estimate, the bulk of the cost of the system is the light projection source, or the Wintech PRO6500 optical engine. Without this component, the liberal cost of the system including spare parts and material is \$1,157.08. When scaling the system into a linear array of duplicate systems, the cost would moderately drop. An additional large cost factor for the DRUM system is the linear actuator used in the prototyped model. This linear actuator with built in motor and control was chosen to reduce the amount of parts and lessen the complexity of the development of the control system, but can be reduced to a fraction of this cost, especially in scaled models. The most crucial component in scaling up the system is the light projection source, as the other

components may be lengthened or connected in series to achieve the same control as the prototype model. Although the PRO6500 provides superior resolution, the scaling of the system may require the light projection system to have a lower resolution or processing capability to make more economical.

3.7 Testing and Evaluation

The initial qualitative testing of the printer functionality was conducted using a commercially available resin (B9-Black, B9Creations, Rapid City, SD.) This resin was used as a conceptual verification as the material had a known print optimization of wavelength and light intensity parameters. The color of the resin also allowed for better visual verification of effective photo-crosslinking as the black resin stood in stark contrast from the HDPE collector shaft it was cured onto. All resulting structures printed throughout the printing testing can be seen in [Figure 3.5](#). Five samples were printed: one printed using the B9Creator layer-by-layer process to compare mechanical properties to radial-layered samples, and four radial-layer samples to aid in understanding the printer dynamics. [Figure 3.5a](#) represents the images displayed by the digital light projector and [Figure 3.5b](#) represents the actual 3D printed sample created by the above projections, respectively. Visual inspections of form accuracy such as radial, median, and cross-section deviations are covered for the various samples.

The sample (i) was created using the B9 Creator, layer by layer, at a dimensional resolution of 30 μm . This print process was approximately 3 hours. The sample has a relatively smooth surface finish with good dimensional accuracy. Individual print layers were distinguishable along the outer wall. The print was also radially symmetric to less

than 0.1 mm deviation between the x- and y-axis and no deviations along the median line or cross-section.

Sample (ii) was the first print attempt utilizing the DRUM printer. Due to the COVID-19 pandemic, proper manufacturing of the original High-Density Polyethylene (HDPE) drums was not possible. This first test of the DRUM printing used a polylactic acid (PLA) drum manufactured through fused filament fabrication (FFF). The exposure projection was a static cube to print a cylinder. As can be seen in the figure, the crosslinking to the drum was ineffective and no final part was formed on the surface of the drum. Different drum submersion depths and a variety of stepper motor speeds were tried. Prolonged exposure with a UV pen was able to grow a very small layer. No cured resin pieces were found in the VAT so we knew our issue was not build-plate adhesion which is a common occurrence for DLP printers. This meant a couple of issues were possible, either the resin fouled or the acid in the PLA was negatively affecting the cross-linking of the resin preventing curing.

Sample (iii) was the first print created using the originally planned HDPE drum. The holes drilled through the midline of these drums were not guaranteed to be straight and mainly caused the drum to visually wobble as it rotated. The exposure pattern started as a wide rectangle covering the majority of the drum and then was shrunk down to a smaller square a few minutes after the print began. This print shows that we are able to create stepped portions along the drum. The lumpy features were attributed to pre-cured resin on the drum prior to this run. A second reason for non-uniform surface features could be contributed to sublayers, layers underneath the current curing layer, not having fully cured. These layers could go on 2, 3 or more rotations before fully curing and

causing stresses to form within the structure. Additional testing would need to be done, however this effect should only affect larger prints as the radius increases requiring additional time to cure if rotational velocity is held constant⁵⁴.

The fourth sample's (iv) exposure pattern was the same as the second sample (ii). The print was set-up to create a similar shape to be compared to sample (i). The print time was less than 10 minutes. The top and bottom edges were rounded yet well defined. This could be fixed using a gradient pattern image to allow the edges to have higher intensity exposure that would cure the resin more uniformly. Individual print layers were not visible, as expected, resulting in smooth outer walls. Despite the visible wobble of the drum while printing, the cylindrical print was radially symmetric with respect to the true radial axis with deviations less than 0.1 mm between the x- and y-axis. No deviations along the median line or cross-section other than the top and bottom edges were observed.

The fifth sample's (v) exposure pattern were three bands of arbitrary heights. It was observed that the smaller projected cure area resulted in a smaller deposited radial thickness of the cured resin, seen on the middle cured band. The edges of the bands were thinner than the center of the band, however the band edges were well defined with no curing outside the intended pattern. This is due to non-linear properties of the photopolymer. This resin must meet a certain threshold of light intensity to begin curing. Increased light energy on the outer portions of a pattern wall might help evenly build up future patterns.

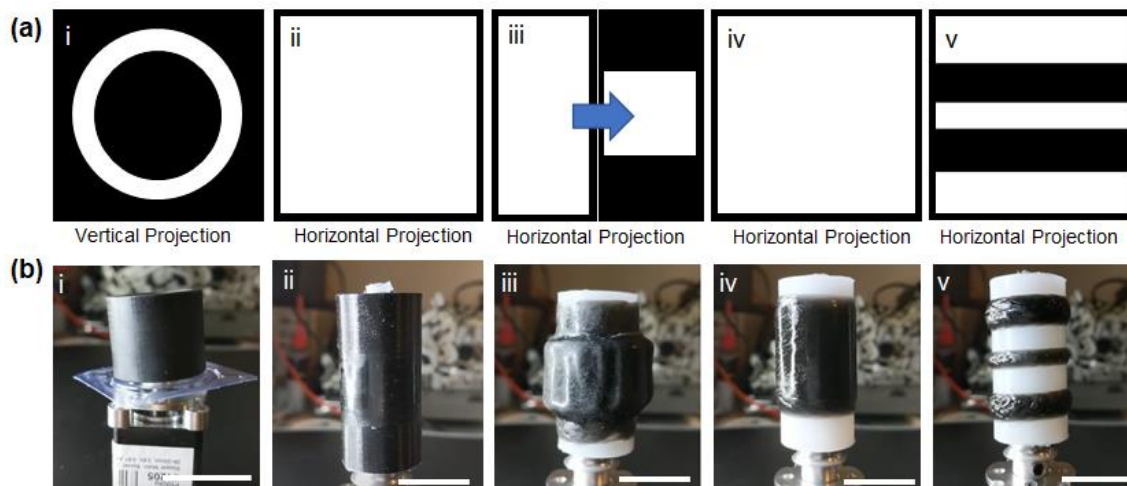


Figure 3.5. DLP printed resin-based structures: (a) patterns of the projected sketch; (b) printed structures: (i) B9 printed (ii, iii, iv, v) DRUM printed. Scale bar: b, 25 mm.

3.8 Discussion

The future work that remains to improve on the understanding and development of the DRUM system revolves heavily around verification of resolution and print geometry accuracy in the rotational collection setup. Studies to identify the rotational speed versus the resulting layer thickness must be conducted to further develop the ability to predict and control layer thickness as a component of the print resolution. Similar to the stripe test previously conducted, a stripe print testing with stripe orientation parallel to the axis of rotation of the collection shaft must be conducted to further understand the effect that the fluid motion exhibits on the print accuracy in the radial direction. This will help to better adjust for the new forces induced from the motion through the fluid pre-cured resin.

After a better understanding of the printing capabilities with the highly defined and easy to visually analyze resin is completed, additional print optimization with a

material suited for tissue engineering GelMA must be conducted. This requires reiteration of the entire optimization process as materials such as GelMA may not behave in the same manner as the black resin. The soft elastic behavior of GelMA may incur significant complexity in print optimization and print accuracy. Having a complete basis of understanding how to tailor the print process to improve the part accuracy on the black resin will create the toolbox required to more intuitively adjust the GelMA printing.

As a proof of concept for adjustment in the layer organization of UV curing systems, we were able to prove its possibility. Significant optimization will be required for full application, both in the development of the system dynamics and the understanding of the flow and materials interactions. This platform allows for the components to be separately sterilized and utilized, making it an ideal layout for studies in biosafety cabinets. It also has been designed such that the collection base is modular and interchangeable with different collection heads as needed. The structural component of the printing system that houses the collector would in theory be able to be sterilized and maintained in the biosafety hood, while the resin bath can be replaced as needed with the desired vessel type. Finally, the UV projection method allows for a distance between the projector and the curing location, which gives the possibility for the UV source to be housed outside of the biosafety cabinet, removing the possibility of contamination from the cooling fans and other components. Though this idea provides great potential, significant characterizations and adjustments are required for ease of use and proof of effectiveness.

CHAPTER 4: BIOMATERIALS STUDY FOR PHOTOLITHOGRAPHIC TISSUE ENGINEERING APPLICATIONS

4.1 Introduction

As has been previously hypothesized, stereolithography or other photolithographic methods may provide a platform in which tissue engineering procedures can be scaled for mass production purposes. This form of growth enablement would not only benefit cellular agriculture but also the medical field and its accessibility and robustness. In light of the suggested method for orientation alteration for scaling, it is crucial to understand, study, and optimize the materials used in these systems.

One key opportunity photolithography may provide is that of chemical crosslinking of these soft materials, rather than physical crosslinking. Physical crosslinking is controlled by weak bonds such as van der Waals bonding while chemical crosslinking utilizes covalent bonding or the sharing of valence electrons- which requires more energy to break. For the case of crosslinking of a material such as a hydrogel or resin, this can result in increased stiffness or thermal resistivity of the material. This is a powerful optimization tool as it can allow you to tailor your material under desired environments to more effectively imitate the behavior required for phenomena such as physical stimuli for tissue maturation.

Luckily, a material's molecular composition can be modified to improve upon the crosslinking. GelMA is a very common example of this in biomedicine and tissue

engineering, made of a gelatin functionalized with methacrylic anhydride, which allows for the cross-molecular bonding when radicals are introduced in the material to induce this reaction²⁴. Though it seems the answer to optimizing control of the material would be to maximize these functional groups, the trade-off is the effect the groups' presences has on the material as a whole for the defined application. These functional groups, as well as the initiators of the radicalization and crosslinking can be toxic to cells and often are not recognized as safe for consumption, but with some products there is limited data which again limits the ability to determine safety. In example, Methyl Methacrylate in this system has been reported by the World Health Organization as a low toxicity and not a carcinogenic factor in rat testing but limited human testing is available⁵⁵.

Not only is temperature a factor to be considered for bioreactor applications, but also the chemical stability under other forces such as degradation by solution or enzymatic or cellular digestion throughout the life of the scaffold. This degradation is exhibited by the breaking down of the molecular structure of the material into smaller molecules of the same material or by-products that are chemically distinct from the mother material. Depending upon the penetration into the system and the mechanism for degradation, degradation can be a regional phenomenon within the material and may alter the overall behavior and toughness of the material with time, compromising the structural integrity.

4.2 Motivation

The goal for material development in this project is to conduct materials characterization on potential candidates for tissue engineering with photolithography to

determine their applicability, particularly in mechanical behavior of the raw material in the biomaturation phase of tissue development. With these pilot studies, two sub-projects were determined, upon availability of resources. The first objective of this study was to compare the compressive behavior of GelMA, a widely used biomaterial in cellular biology, with traditional meat products to provide to determine its direct application in cellular agriculture. The second determined objective upon completion of the GelMA characterization was to investigate the degradation of a soy-based biodegradable resin while aging in solution. With these studies, we aim to shed light on the complexity of the development of these tissue engineering systems with an in-depth discussion to follow.

4.3 GelMA Compression Study

The first material to be investigated in this work for its use in photolithographic biomedical and edible applications was GelMA. In the following subsections, the protocols followed will be described for each step of the experimental process. Following the outlined materials and methods, the results will be presented and a brief summary of the work with this commonly used biomaterial. The further discussion of this work will be located in the such-titled section of the overall chapter. The primary objective of this study was to determine if GelMA at printable concentrations is capable of directly imitating native meat tissues in compression.

4.3.1 Materials and Methods

GelMA Synthesis

GelMA was synthesized following a protocol that has been reported previously⁵⁶. For the synthesis, gelatin (Porcine, Type A, 300g Bloom, Sigma Aldrich) was dissolved in

phosphate buffered saline (PBS, P3813 Sigma Aldrich) at a 10% w/v ratio. Then methacryloyl anhydride (MA) (Sigma Aldrich, St. Louis, MO) was mixed dropwise with the dissolved gelatin at 1.25%(v/v). Upon completion of the reaction, the solution of the gelatin, MA, and PBS is diluted to 5X PBS total ratio to halt the reaction. The diluted solution was transferred and dialyzed in 12-14 kDa molecular weight cutoff tubing in deionized water to remove the nonreacted methacrylic anhydride for 5-7 days. The dialyzed GelMA solution was then lyophilized at -80 °C for one week and stored for future use.

GelMA Hydrogel Preparation

Freeze-dried GelMA was dissolved in PBS at predetermined weight to volume concentrations, of 7% and 10% - determined as optimal from pilot studies not included in this report- and the photoinitiator lithium acylphosphinate salt (LAP) (Allevi, Boston, MA) was added at 0.067% (w/v)⁵⁷. Tartrazine was incorporated as a photoabsorber at concentrations of 0 and 2.25 mM²⁹. The pre-crosslinked solutions were placed in 90 mm uncoated petri dishes and cured in bulk at curing times of 30, 60, and 90 seconds using a 405 nm pen light at a distance of 10 cm from the surface of the hydrogel. Post-curing, samples were punched from the bulk material to be tested in uniaxial compression with final dimensions of 15.875 mm diameter and 4 mm thickness. Four samples were prepared for each concentration and curing time. All preparation and testing were conducted at 22.5 °C room temperature. A depiction of this process as well as an example of the sample geometry can be seen in [Figure 4.1](#).

Meat Sample Preparation

To determine the applicability of GelMA for the edible tissue context, multiple meat and fish varieties were chosen to cover a range of mechanical behaviors desired. The meat products were frozen at -20°C for 48 hours before slicing to a uniform thickness of approximately 5 mm. Samples were punched from these sheets using the same diameter punch as the GelMA samples with a diameter of 15.875 mm. All samples were allowed to reach room temperature before testing. The species investigated were sourced from a local meat market and include: tilapia filet (TF,) scallop (SC,) pork tenderloin (PT,) chicken breast (CB,) and sirloin steak (SS.)

Uniaxial Compression

Uniaxial compression testing was conducted on the Cellscale UniVert, displacement controlled with a displacement distance of 3 mm with a displacement time of 20 seconds, followed by a 5 second hold to allow for hysteresis to be graphed, followed by a recovery displacement of 3 mm in 20 seconds, the same rate as the loading phase. The resulting force was recorded at a sample rate of 5 Hz and plotted with respect to the experienced strain, normalized by the initial thickness determined as the z-distance between the parallel plates upon first recognition of a reactionary force from the force sensor.

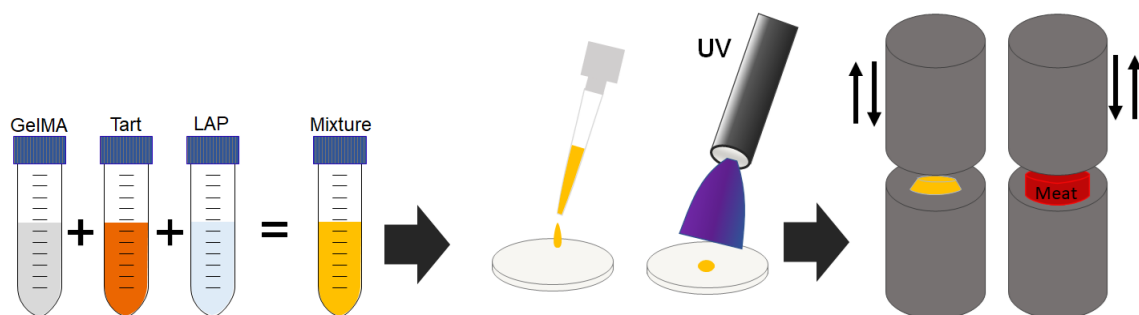


Figure 4.1 Depiction of the Mix, Cure, and Test of compression samples.

4.3.2 Results

All compression data was compiled and compared. The adjustments of the defined variables as well as the similarity of the optimal hydrogel solution was compared to the tested meat samples. For reference, [Table 4.1](#) describes the abbreviations used within the results of the depicted in the figures. [Figure 4.2](#) shows the effect of variation of hydrogel preparations. In [Figure 4.2a](#), the effect of curing time can be seen. As the curing time is increased, the elastic modulus of the sample was increased, depicted by the slope of the curve upon loading. The resultant stress per strain also increases with respect to increasing curing time, where a stress of 40 kPa was achieved at a strain of 0.48, .56, and .62 for 90, 60, and 30 seconds respectively. In [Figure 4.2b](#), the modulus is increased with increasing GelMA concentration from 7% to 10%. Finally, when tartrazine is adjusted from 0 to 2.25 mM concentration, the moduli are decreased, consistent across all curing times seen in [Figure 4.2c](#).

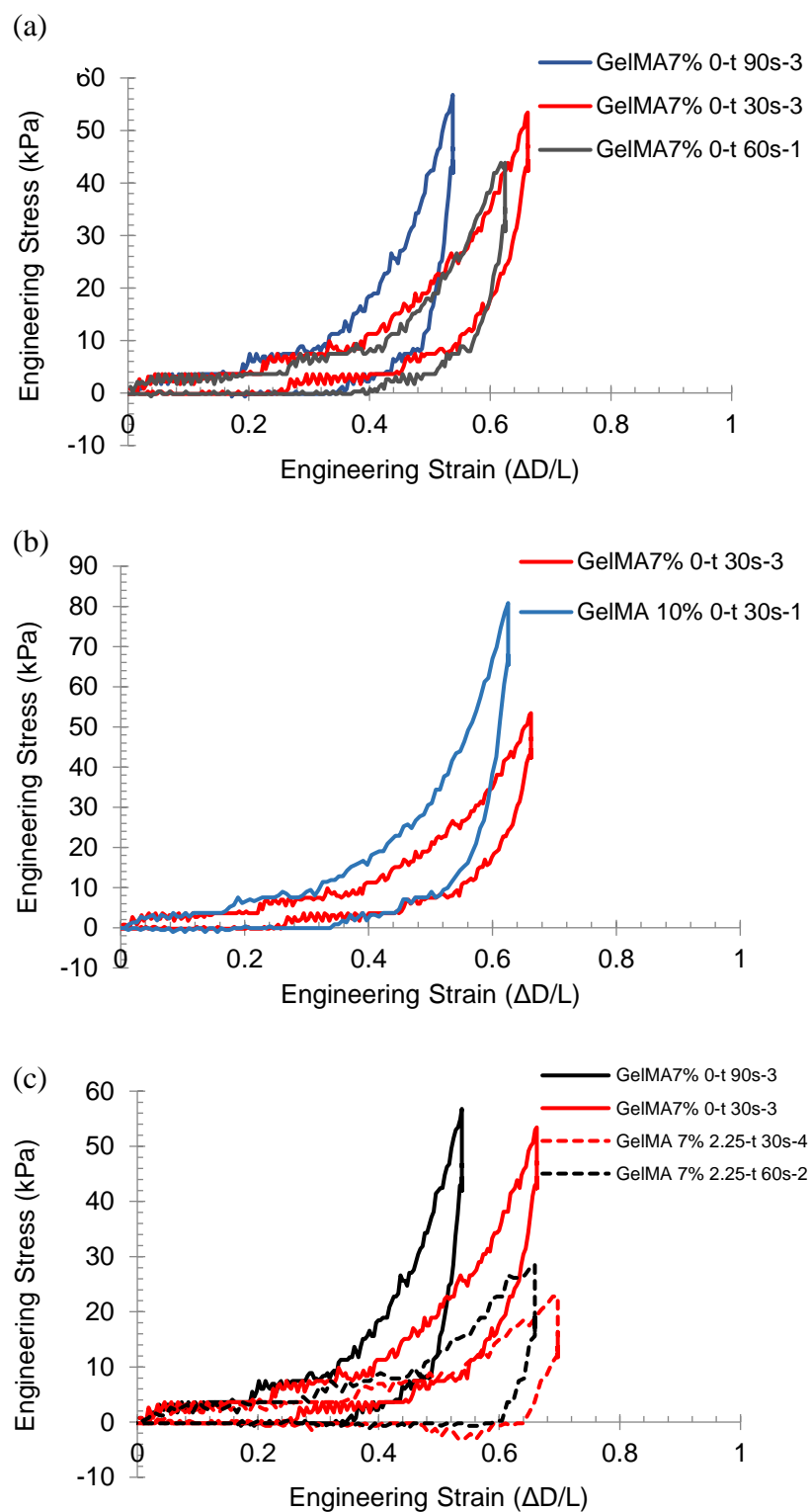


Figure 4.2 Variation of hydrogel concentrations and treatment. The engineering stress strains plotted, where the adjustment in (a) curing times, (b) GelMA concentration, and (c) tartrazine concentration are identified.

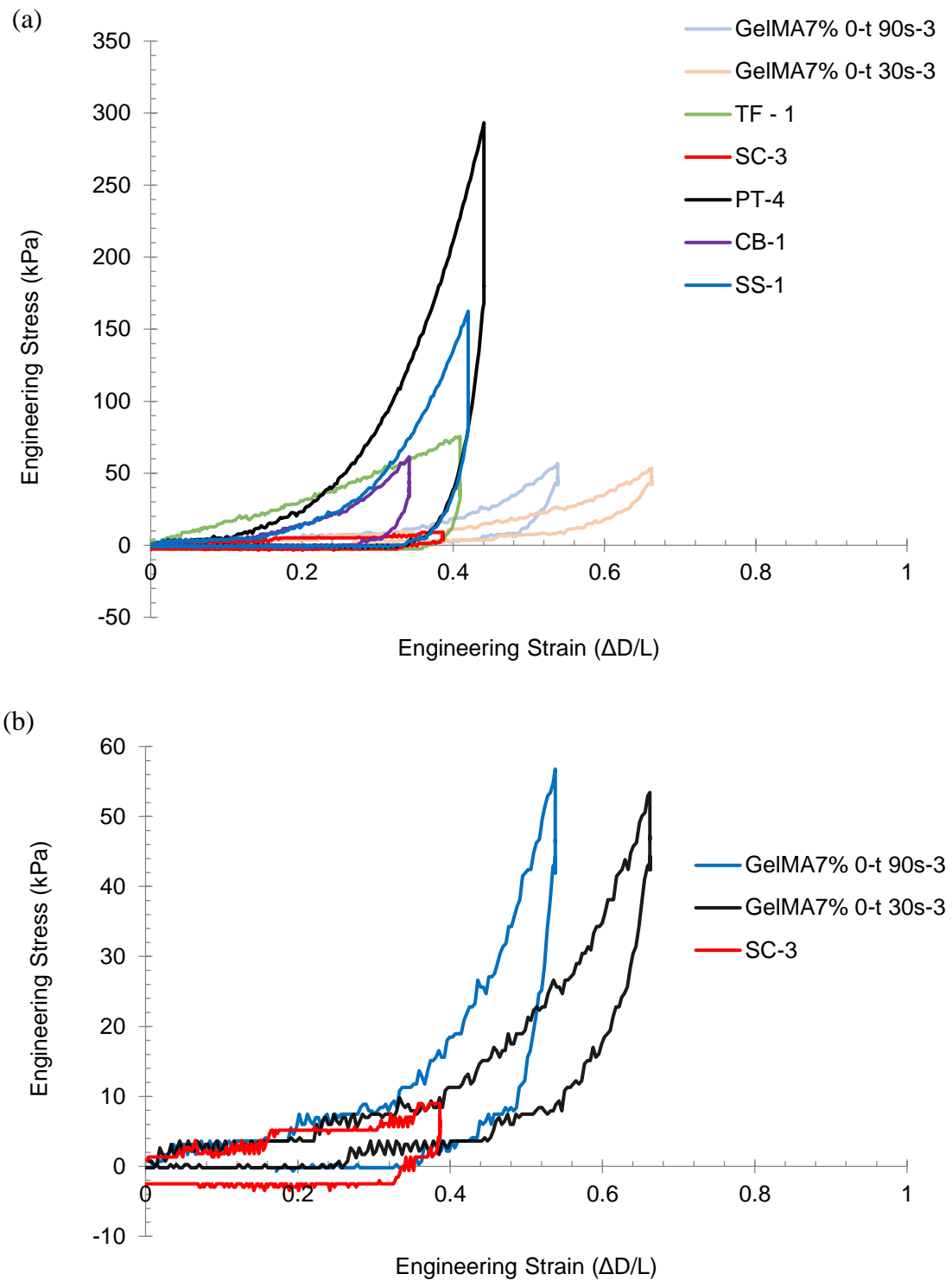


Figure 4.3 GelMA and Meat Tissue. Engineering stress-strain curves of GelMA 7% with 0-tartrazine compared with (a) all meat tissue samples tested, and (b) an isolated comparison with scallops for further discussion.

After determining the overall effects of the variation in concentrations and curing time, GelMA at 7% concentration with no tartrazine was determined to be an optimal formulation as it flowed more easily than that of the GelMA 10% and had higher crosslinking than that with tartrazine and therefore a higher modulus. This formulation was then compared with the meat tissue samples to determine the natural similarities with the raw products at room temperature, if any. **Figure 4.3a** shows this formulation at curing times of both 30 and 90 seconds as well as the curves for all tested meat samples. The GelMA samples show little correlation with the bulk of the tissues tested. The most applicable tissue was determined to be the scallops, as seen in **Figure 4.3b** having similar initial stress-strain behavior to that of the GelMA with the 30 second cure time. This can be identified as the largest limiting factor for GelMA photolithography as a direct implementation in food engineering systems.

Table 4.1 Sample Nomenclature for GelMA compression results

Abbreviation	Sample Source (raw, room temperature)
TF	Tilapia Filet
SC	Scallop
PT	Pork Tenderloin
CB	Chicken Breast
SS	Sirloin Steak
GelMA 7% 0-t 90s	GelMA 7%, no tartrazine, 90s cure
GelMA 7% 0-t 30s	GelMA 7%, no tartrazine, 30s cure

4.3.3 Summary

Multiple concentrations of GelMA hydrogel were tested in uniaxial compression in displacement-based control. These were directly compared with samples of raw native

tissue typical for consumption. Based on printability constraints and the observed native tissue behavior, GelMA at 7% concentration with no tartrazine and 30 seconds curing time was the most similar in mechanical response to compression testing as that of a native tissue- particularly raw scallops. Multiple conclusions can be drawn from this, but namely that GelMA alone in this concentration is not sufficient for achieving the range of mechanical behavior desired for different imitative meat textures. This leads to a need for additional materials to be considered, either supplementary or complementary, for the optimization of the system.

4.4 Bio Soya Resin Degradation

Following the investigation of GelMA for photolithography of meat tissue, an additional potential photocrosslinkable material was determined to be biosoya 1. This material is commercially available and would be used on the basis that it will degrade over the time of the biomaturation process, theoretically leaving only a matured tissue upon completion of biomaturation. In addition, this material is soy-based rather than animal gelatin, which could provide a more sustainable supply chain for cellular agriculture or the reduction of reliance on animal slaughter. The primary objective of this study was to characterize the degradation of a soy-based photolithographic resin to validate its applicability in cell-culture use, like depicted in [Figure 4.4](#). The crosslinking range of the biosoya was first characterized to develop a baseline of expectation for the material. After the baseline is determined, the degradation of the material was tested via aging in solutions which are relevant to biomaturation and cell culture environments. The

results of these studies were then collected and evaluated for its potential use. Further discussion of this study can be found in the Discussion section of this chapter.

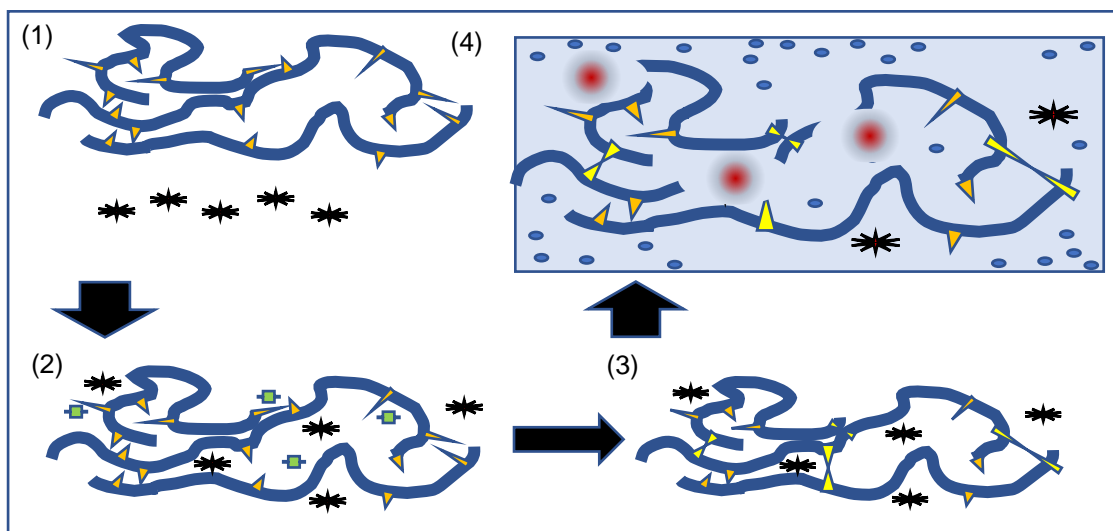


Figure 4.4 Schematic of degradation in which (1) the functionalized photocrosslinkable resin and enzyme are mixed, (2) the material is exposed to UV, creating radicals in the material. (3) These radicals initiate crosslinking between the functionalized molecules. (4) Upon submersion in solution, the material degrades with the enzymes serving as a catalyst to the degradation of bonds.

4.4.1 Materials and Methods

Resin Formulation and Sample Preparation

Biosoya 1 resin was purchased from 3DResyns (Bio Soya 1 resin – Clear, P11892/2I, 3DResyns, Spain.) This resin is soybean-oil-based and formulated for MLC D printing, with a z-resolution of 50 to 100 μm . Biosoya has also been developed to be compatible with an enzyme supplied by the same company to increase the rate of biodegradation of the material. This enzyme, 3DResyn-ase EBC-1, is added into the pre-cured resin, and increases the rate of hydrolytic and bacterial degradation the material

experiences. For degradation studies, directly prior to printing, the enzyme was added to the resin base at a weight ratio of 0.5% then thoroughly mixed. All samples were printed using Anycubic Photon S. An initial qualitative layer adhesion analysis – not included in this report - was conducted to determine the range of exposure times to be tested throughout our studies, with the minimum exposure time to be defined as 10 seconds with significant accuracy loss, and 13 seconds with near net accuracy to the designed structure. The utilized curing times are reported for each sample tested as a tracked variable.

Testing Plan

An initial investigation was conducted to characterize the crosslinking kinetics and optimal exposure times per layer of the material at 50 μm layer thickness. Two sample types were prepared, and all data points are depicted in **Table 4.2**. The first set were cured droplets of 100 μL of resin, placed into the Anycubic Wash and Cure 2.0 for a range of 0 to 60 seconds. The purpose of this data set was to allow for the characterization of the crosslinking evolution over a wider range than is possible in the printed system, as there is a lower limit of crosslinking to achieve successful adhesion to the build plate. The second sample set was printed using the Anycubic Photon S, with sample dimensions of 12 mm x 2 mm x 60 mm, with the 12 mm dimension in the orientation of the z-direction of the build. The cure droplets were characterized by differential scanning calorimetry and infrared spectroscopy to verify the successful crosslinking limits of the material, while the printed samples were similarly tested with the addition of dynamic mechanical analysis to characterize the evolution of mechanical

behavior with respect to the applied exposure times. These pilot studies will serve as a baseline for the degradation experimentation to follow.

To directly quantify and understand the crosslinking behavior and effect of degradation within the material- thermo-/mechano-/chemical behavior. This can be measured through a careful planning of experimentation, with multiple physical principles at different times and in different environments. The degradation parameters studied and the protocol followed are directly described in the following section.

Triplicates for each unique parameter combination were prepared and placed under the specified environments. Upon the completion of the degradation time for each sample, tests were conducted to validate the degradation both chemically and mechanically. For chemical degradation analysis, infrared spectroscopy, differential scanning calorimetry and pH variations were collected. To determine mechanical degradation, studies were conducted via dynamic mechanical analysis and swelling tests.

Table 4.2 Nomenclature for non-enzyme soya resin samples

Sample Name	Preparation method	Layer Exposure (sec.)	Post-Curing Exposure (sec.)	Heat Treatment 200 °C
UCR	Uncured resin	-	-	-
CD3	Cure droplet	-	3	-
CD15	Cure droplet	-	15	-
CD30	Cure droplet	-	30	-
CD60	Cure droplet	-	60	-
PS13	Printed sample	13	-	-
PS13C5	Printed sample	13	300	-
PS13H5	Printed Sample	13	-	300
PS30	Printed Sample	30	-	-
PS30C5	Printed Sample	30	300	-
PS30H5	Printed Sample	30	-	300

Table 4.3 List of tests and time points utilized in degradation analysis

Test (all conducted in triplicate)				
Day:	DMA	Swelling	DSC	IR
0	x	x	x	x
1	x	x	x	x
7	x	x	x	x
8	x	x		x
14	x	x		x
15	x			x
28				
All Experiments conducted in triplicate				
Repeated for two solutions: Ethanol 99% and PBS				

Aging in Solution

For all degradation points, the experiments described in the following were conducted for each sample. To test hydrolytic degradation of the Bio Soya samples with the added enzyme, a testing matrix was created to determine the sample and environments required. This can be seen in [Table 4.3](#). Though no direct standard is applicable for this study as this application of a material is not well defined in the new and currently unregulated field, ASTM F1635-11 was used to inform the development of the protocol. Two environments were used to test long-term degradation.

These samples were placed in 99% purity ethanol or phosphate buffered solution at 37°C, chosen as the temperature used for bioreactor operations with its similarity to the typical body temperature. Phosphate buffered saline solution was used as a pH balance for the solution during degradation to minimize pH variation effects on the degradation process, according to the aforementioned ASTM standard. Though PBS is the ASTM standard, ethanol was used for additional testing. Ethanol provides exaggerated swelling due to molecular compatibility with acrylates, and can cause damage to the polymer

chains, leading to stress cracking⁵⁸. It was also determined to reduce the effective life of other enzymes used to degrade acrylated polymers⁵⁹. Not directly given from the manufacturer, this resin is likely acrylated soy, due to the reported by-products from bio-enzymatic degradation - methane, carbon-dioxide, and water. This, in addition to the likely exaggerated swelling, will also provide additional evidence to suggest the functionalization used on this soybean oil-based resin. Each sample set was immersed in, at minimum 30:1 ratio of solution, with our target ratio of 50:1 solution to sample volume ratio. Samples were placed in the same vessel for each time point for consistency between samples between different testing protocols. The vessels were tightly sealed to inhibit outside contamination or evaporation of byproducts or the solution.

Thermogravimetric analysis

To investigate the thermal stability of the Bio Soy1 polymer resin in extreme cooking temperatures or prolonged exposure in a bioreactor, thermogravimetric analysis (TGA) was conducted using a TGA Discovery. Samples of approximately 5 mg were collected from three points to characterize the TGA variation as a function of ultraviolet (UV) crosslinking or UV exposure time. The first point tested was the polymer resin with no UV exposure. Printed samples were conducted at two exposure modes: 13 seconds per layer with no additional post-curing, as well as an over-exposed sample at 13 seconds per layer and a 5-minute post-print curing cycle. The choice of samples was to determine the influence of the exposure time on the cross-linked state of the resin. All samples were heated from an initial temperature of 30°C up to 600°C at a temperature ramp of 10 °C/min. The pressure of the system was maintained at 0.5 bar and the percentage weight

loss was recorded as a function of the degradation temperature. This was repeated for the samples with and without enzyme present and used to inform the temperature ranges in differential scanning calorimetry and dynamic mechanical analysis.

Infrared Spectroscopy

Infrared (IR) spectroscopy was conducted on a ThermoScientific Nicolet iS10 with Smart iTR to investigate the absorption at various UV exposure times. A difference in infrared spectrum between samples implies modification of chemical bonds inside the resin as well as the ability to be further crosslinked. An initial test was conducted on the least cured resin droplets (CD3) and the most cured resin droplet (CD60) to set a control for measurement. Multiple tests for chemical variation throughout printing, incorporating the enzyme, and thermal cycling up to 200°C were conducted.

Differential Scanning Calorimetry

To further define the structural changes when heated to cooking temperatures, differential scanning calorimetry (DSC) was conducted on a TA Instruments DSC Q100 that was calibrated using Indium and Zinc reference materials. An initial test was performed using 500 μ L droplets of resin cured in the Wash and Cure 2.0. This study was conducted to characterize the range of curing kinetics and determine the range in which the printed samples' stiffness can be obtained within the curing curve. During DSC analysis, the samples were cooled to -80 °C and held in an isothermal state for 1 minute to reach equilibrium before being subjected to a temperature ramp from -80 °C to 185 °C at a rate of 20 °C/min, under nitrogen flow at 50 mL/min. The resulting heat flow curves

were collected for the investigation of the evolution of the microstructure of crosslinked thermoset and its stability. This protocol was repeated for printed samples both with and without the presence of the enzyme, to ensure for controls in analysis.

Dynamic Mechanical Analysis

Dynamic mechanical analysis was conducted on a TA Discovery DMA 850. Samples with a geometry of 2 mm × 12 mm × 60 mm were printed with given exposure profiles with the width of the sample along with the z-layer orientation of the printer. Samples were loaded under displacement controlled 3-point cantilever orientation in nitrogen gas and subjected to a heating rate of 2 °C/min from -55 °C up to 120 °C. The displacement was 30 μm at 1 Hz. The temperature limits were chosen based on the glass transition results from DSC. The corresponding loss moduli were analyzed to further identify the phenomena of crosslinking and degradation seen in the thermomechanical behavior.

Swelling

Swelling of the samples in solution were conducted by analysis of weight difference between the saturated sample directly removed from the solution and the dried sample weight. The samples were allowed to dry for two weeks from removal from solution prior to final weighing. This was determined an adequate drying time as the percent weight change from day-to-day was less than 5 milligrams, which was approximately 0.5% of the total weight of the sample. After measurements were

collected, the following equation was used to calculate the percent swelling of the solution into the sample as weight ratio of solution to sample mass.

$$\%W_{swell} = \frac{W_{wet} - W_{Dry}}{W_{Dry}} \times 100\% \quad \text{Eq. 3.1}$$

4.4.2 Results

Upon completion of the required testing protocols, the results can be categorized into three stages: the crosslinking analysis, the effect of the addition of the enzyme, and the degradation of the material in solution. Each stage will be presented in the following subsections.

Crosslinking analysis

The first component of characterization was to form a baseline of understanding of the evolution of chemical bonding through the curing process. This was conducted primarily through infrared spectroscopy. **Figure 4.5** shows the infrared spectroscopy absorbances of selected key samples. 3s CD and 60s CD are cure droplets cured for 3 and 60 seconds respectively both in shades of blue. PS 13s and PS 30s are printed samples without enzyme with layer exposure times of 13 and 30 seconds respectively in shades of green. Finally, the black curve is PS+E 15, or the printed sample with incorporated enzyme at 15 seconds per layer exposure.

No in-depth bonding correlation or Hummel analysis was conducted, but a trend in the evolution of absorbance peaks can be seen with the varied sample preparations. When looking at the blue curves or the cure droplets, the steep peak that is seen around

1200 cm^{-1} is significantly reduced with increasing crosslinking. These two samples were chosen to create the maximum and minimum measurable points in crosslinking efficacy of the resin without the enzyme present to depict the extremes not possible in printing, where under curing leads to delamination of layers and overcuring can be damaging to the printing system and reduce the print accuracy, also requiring significant times to print full samples to test.

Turning to the printed samples without enzyme in green, though there is variation in overall intensity due to testing on different days, the curves exhibit the same curve shape as that of the fully cured 60 second cure droplet, leading to the conclusion that both samples are considered fully cured upon printing with low significant improvement between the 30 seconds and 15 seconds per layer exposure time. For purpose of cell culture and power savings, this would suggest the lower range to be optimal as the crosslinking is successful and does not waste additional power, also reducing the exposure to UV, which would improve cell survivability if printing with cells within the resin. Finally, when comparing the printed sample with the enzyme to the previous sample sets, it looks to achieve a middle ground between the fully cured and minimally cured samples. Specifically, the peak that is reduced upon completion of crosslinking still remains in large part and is the second highest absorbance peak on the enzyme incorporated curve. This would suggest that the enzyme is either inhibiting or disrupting the crosslinking efficacy of the resin or the enzyme incorporation allows for new chemical bonds to be present in the material, forming a new peak.

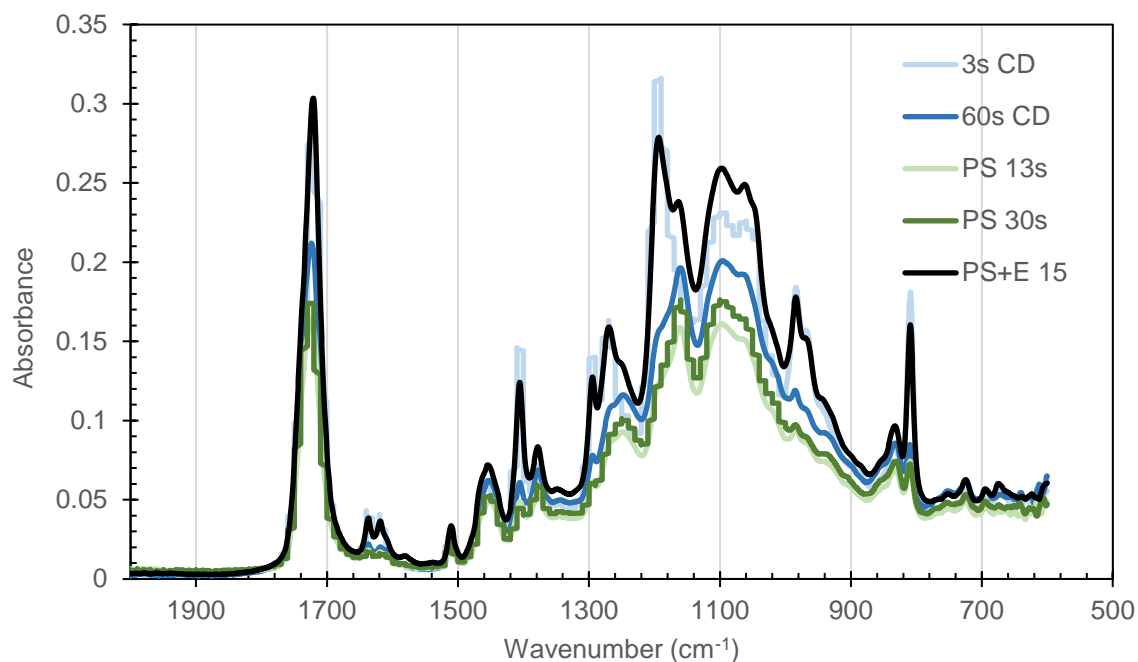


Figure 4.5 Chemical bonding evolution throughout crosslinking process.

Adding the Enzyme

In addition to changing the chemical signature in infrared spectroscopy, the incorporation of the enzyme into the resin base also effects the thermomechanical behavior of the material. As seen in [Figure 4.6a](#), dynamic mechanical analysis was conducted on samples with and without the enzyme present. With the incorporation of the enzyme, seen in blue in the figure, the relaxation peak seen on the loss modulus curve shifts to lower temperatures. This shift of approximately 20°C, as seen between control and control + EBC-1 enzyme data in [Table 4.4](#). At the desired operating temperature, this shift in the curve also results in a reduction in the experienced loss and storage moduli of approximately half a decade, but appears to level out at higher temperature. As this material is much more rigid at room temperature than that of native meat tissue, this is actually likely a highly desired phenomenon.

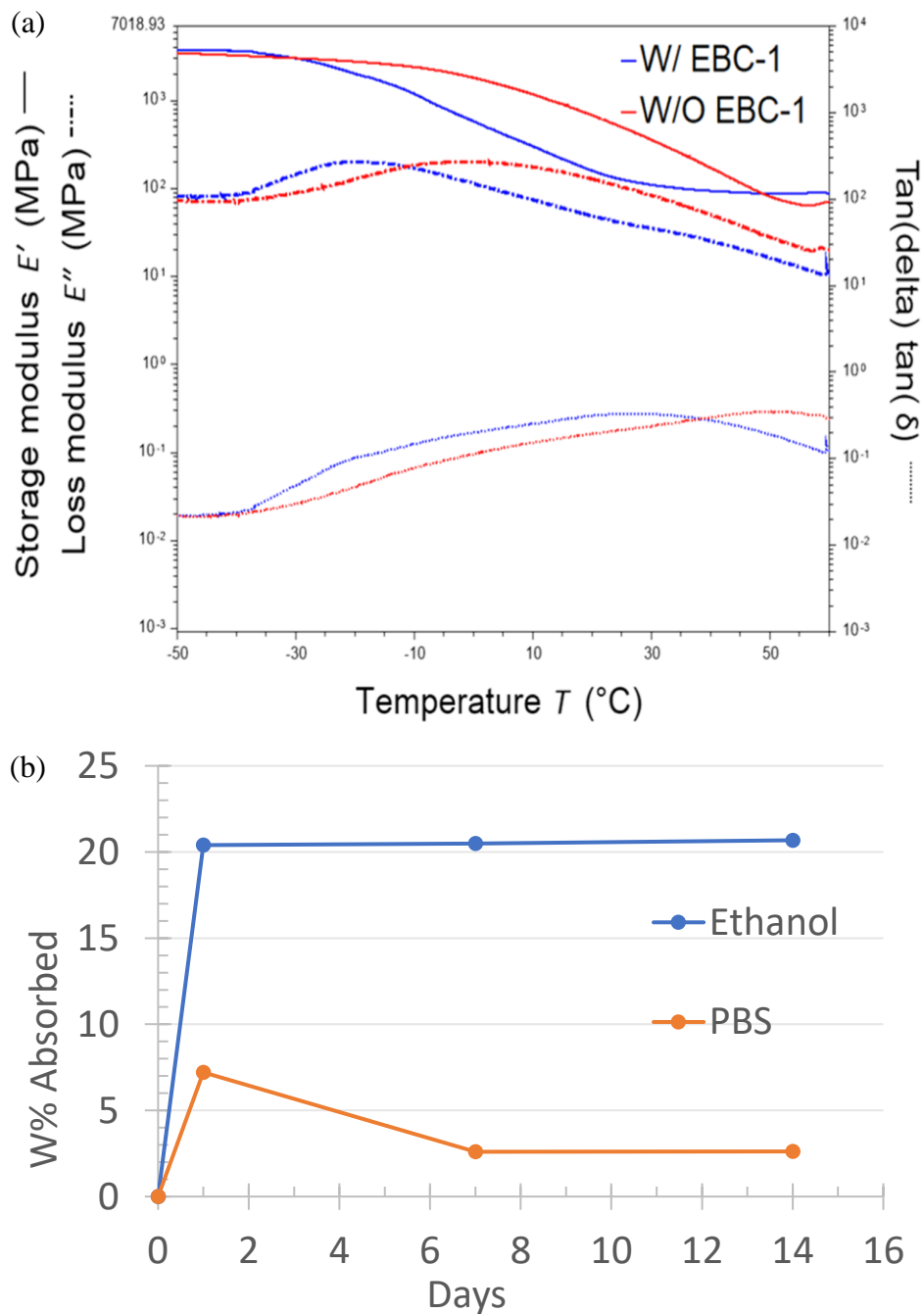


Figure 4.6 DMA of soya with additive enzyme EBC-1 and swelling of soya in solution. (a) storage and loss moduli and $\tan(\delta)$ of biosoya 1 resin with (blue) and without (red) EBC-1 enzyme. (b) graphed swelling in each solution represented as %w of solution absorbed to sample weight.

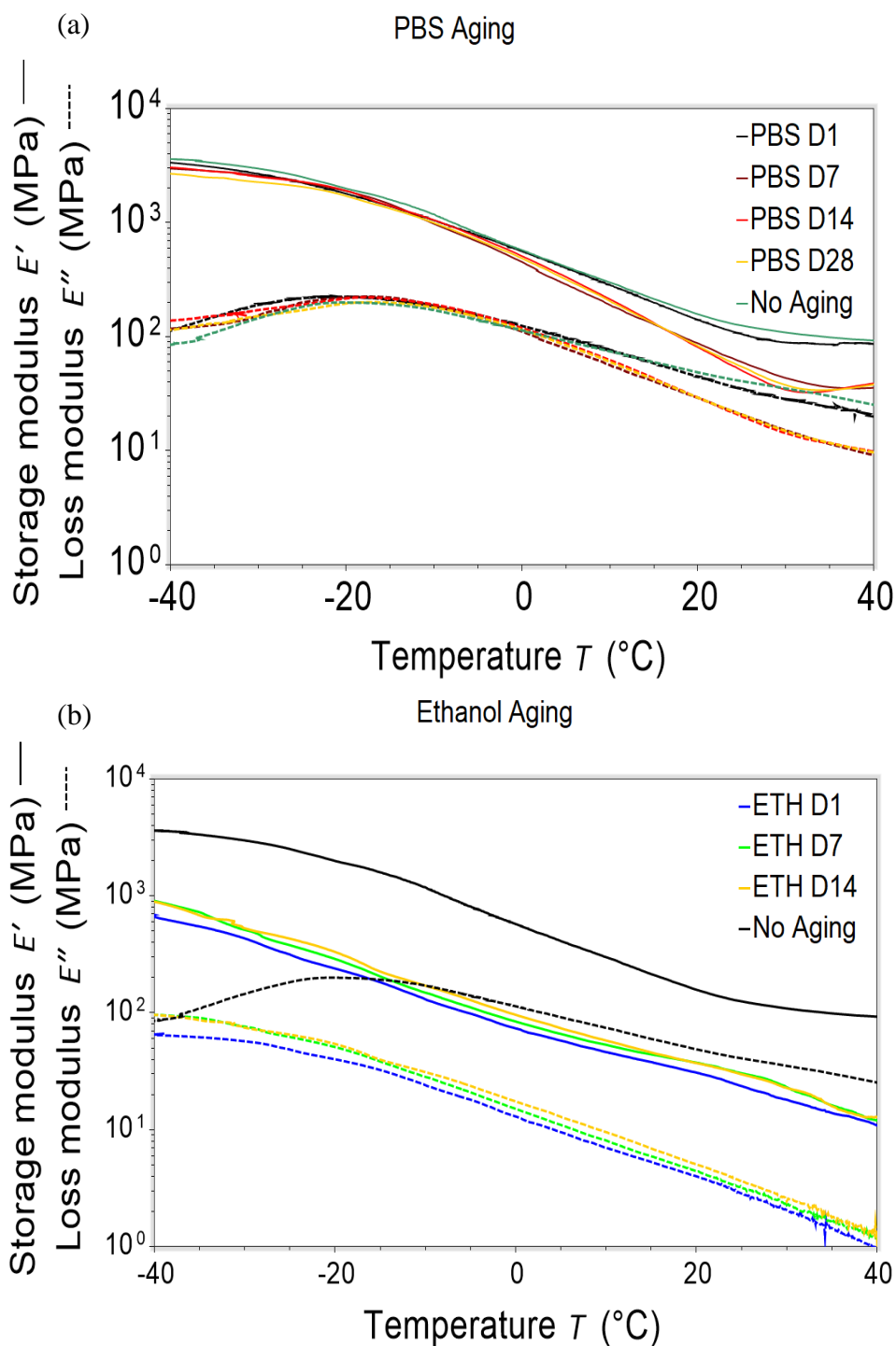


Figure 4.7 DMA of soya with additive enzyme EBC-1 (a) DMA storage and loss moduli evolution due to ethanol aging, with no aging (black) as reference. (b) DMA storage and loss moduli evolution due to PBS aging with no aging (green) as reference

Degradation

To better quantify the variation in swelling or penetration ability of each of the solvents at the testing temperature within the material, the simple swelling test was conducted and recorded, as can be seen in **Figure 4.6b**. As evident in the graph, ethanol (blue) had a significantly higher absorption rate into the samples, just over 20% by weight of the dry sample. PBS on the other hand had a maximum absorption of 7.2% at Day 1, then leveling out to 2.7% by weight at Day 7 and on, just over 33% as much as that of ethanol. The effect this difference in penetration and further degradability can be seen in the aging in solution of ethanol and PBS in **Figures 4.7a and b** respectively.

In ethanol, as the aging increased there was a reduction in moduli at each temperature point throughout the test window. This could either mean a direct reduction in moduli or possibly a shift of the moduli relaxation phenomena to lower temperatures, which could be investigated with Time-Temperature-Superposition or widening the testing temperature window. The storage modulus is reduced by nearly one decade throughout the entirety of the testing window, whereas the loss modulus seems to lose its characteristic relaxation peak at -20.8°C . The most severe change in behavior was experienced between no aging and Day 1, as ethanol quickly penetrates the system and exhibits plasticization and potentially degradation by Day 1. In particular, the storage moduli quickly reached approximately 14 MPa and remained while the loss modulus was reduced to approximately 1.4 MPa. In PBS, the most significant change to the behavior was experienced between Day 1 and Day 7, where there was a drop in storage modulus of 60.0% at the desired operation temperature of 37°C . This change was only experienced

after the relaxation peak at -17.6°C , which remained constant throughout aging in PBS after an initial decrease of approximately 3°C .

Table 4.4 Key Moduli and Peak Relaxation for Aged Samples

Solution	Day	Storage Modulus G' (MPa) at 37°C	Loss Modulus G'' (MPa) at 37°C	Tan(δ) at 37°C	Relaxation Peak Temperature ($^{\circ}\text{C}$)
Control (C)	0	216.5	59.7	0.28	-1.19
(C +EBC-1)	0	95.8	28.1	0.29	-20.8
PBS	1	88.2	23.1	0.26	-21.0
	7	35.3	10.4	0.30	-17.6
	14	40.9	11.8	0.29	-17.73
	28	35.3	10.8	0.31	-17.42
Ethanol	1	13.0	1.2	0.09	-
	7	14.5	1.5	0.10	-
	14	13.9	1.6	0.12	-

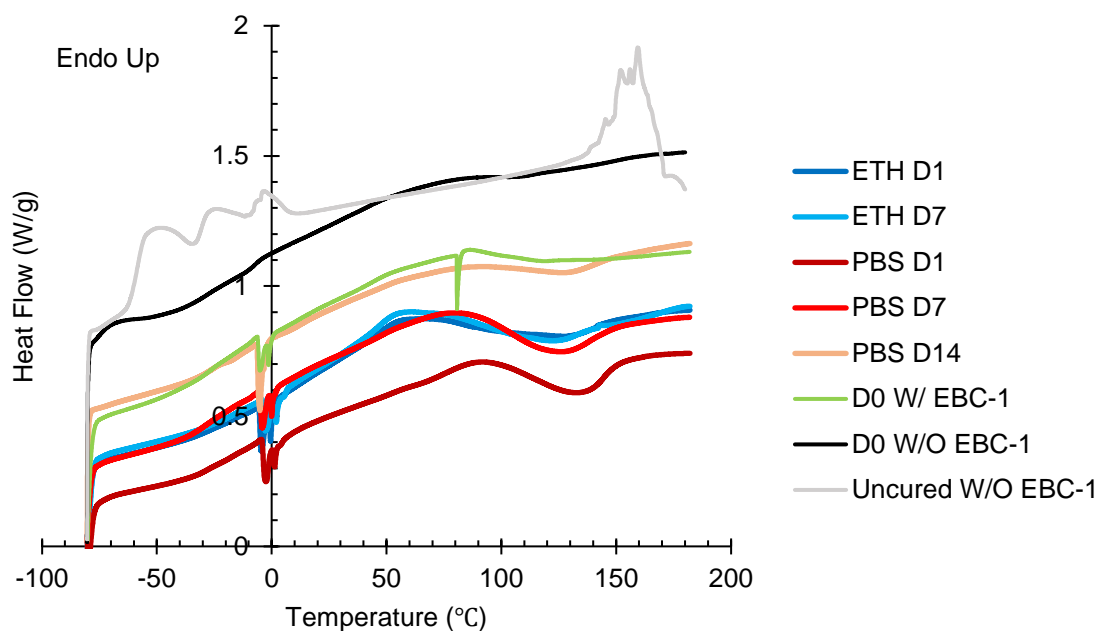


Figure 4.8 DSC Analysis of soya degradation combined graph, normalized.

The results from the DSC tests were collected and graphed together in [Figure 4.8](#) for analysis of the variations in thermal behavior of the samples. For a control without

enzyme incorporation, a grey scale reference curves of the resin without EBC-1 enzyme cured (black) and uncured (grey) was included. Next, the printed sample with EBC-1 before aging (green) was collected to create the additional control for aging. The aging curves can be seen in red for PBS aging and blue for ethanol aging, in which the color saturation decreases with increasing aging time.

Regarding the printed samples without EBC-1, the effect of curing, from liquid resin to fully cured resin is quite apparent. In the uncured resin, the wavy portion in temperatures between -55 and 10°C is likely due to inconsistencies from the nature of the material in liquid form, including any adjustments from air pockets, and smaller localized reorganization in the material. There is additionally an endothermic peak with an onset of approximately 140°C, which could be a melting of the oriented structure attained from reorganization at the lower temperature range or is evidence of the beginning of thermal degradation, especially due to the rugged multi-peak structure and following endothermic hump around 170°C. Upon curing, these phenomena are no longer present in the thermal signatures of the material, which is strong evidence for effective crosslinking, as the crosslinking between molecular chains inhibits reorganization, including crystallization or melting. A wide glass transition range can be seen at low temperatures with an onset of approximately -50°C.

Once the enzyme has been added (green,) a new crystallization peak can be seen at approximately -5 to 0 °C. As many enzyme solutions can be co-enzyme systems, a simplification in our analysis had to be made in assuming one primary enzymatic presence for the sake of thermal presence, that of likely an amide enzyme⁶⁰. The presence of this enzyme, therefore can be seen by the addition of the exothermic crystallization

peak of the amide functions able to reorient within the material samples. An additional endothermic spike was recorded at 78°C, but this is likely an artifact and bears no significance to the characterization and understanding of the thermal behavior of the sample. It is interesting to note, however, that this occurs in the same temperature range as the other variations between non-enzyme and enzyme samples. In addition, upon aged samples there exists an exothermic curve, present in the non-aged but more exaggerated in the aged samples experienced between 80 and 150 °C. This is likely evidence of crosslinking or a recovered ability to reorganize, such as recrystallization potentially aided by the presence of the enzyme throughout that can serve as nucleation points.

4.4.3 Summary

A multi-method approach to characterizing thermochemical and thermomechanical behavior changes with respect to an enzyme incorporation and further aging in cell culture relevant temperature and solutions. It was found that the enzyme incorporation decreases the peak relaxation temperature and the moduli inherent in the material at the desired bioreaction operation temperature of 37°C. In addition, PBS aging has little effect on the peak relaxation temperature, but decreases the moduli above peak relaxation, particularly at desired temperature. Finally, ethanol has a significant reduction in moduli or shift towards lower temperatures as strong evidence for plasticization, seen by Day 1 of the aging in solution period.

4.5 Discussion

Through each study, none of the suggested materials are stand-alone answers to achieving the proper mechanical behaviors in their respective modes. Compared with a recent study⁶¹, the range of storage and loss moduli typical for poultry and sausage products are 25 to 40 kPa, and 5 to 8.5 kPa respectively. The pure soya resin material is still significantly higher than that of these desired values, but does assume 100% soya product rather than a combination of cellular materials, cell-produced extracellular matrix and proteins, and flow paths required for waste removal and nutrient delivery. The initial GelMA studies are difficult to compare with others in literature as the recent proposed methods for testing cellular agriculture are not simple uniaxial compression, therefore no direct comparisons can be made. In addition, when testing these types of viscoelastic materials, it is crucial to test at the same strains and frequencies to optimize the comparability between the measured behavior.

With respect to adjustments to GelMA for improvement in this application, one of the most optimal methods is to incorporate a secondary material to provide increased mechanical resistance. As suggested in Chapter 3 of this work, one optimal secondary material to create composite structures lies in electrospun fibers. These fibrous mats can imitate similar nonlinear inelastic behavior that native muscle tissues can exhibit, as the alignment of fibers will change with the application of force and increase the resistance. This could offer significant tailorability of the profile across the range of stimuli, rather than at one constant rate. In addition, a further study using textural profile analysis or another method for testing is required to better understand GelMA's behavior over a range of temperatures and loadings.

For soya-based resin, the tailorability and degradability of the base material was investigated and quantified. Significant further studies will be required to continue to optimize this material for cell-culture products. One potential use is in a more hollow printed scaffolding that can either be flooded with a softer material or left open for cells to directly migrate into. One of the biggest drawbacks to the use of this material, though it has desired thermomechanical behavior and tailorability, is its lack of RGD moieties or bonding sites for the cells to attach to. This would again require either additional functionalization of the material to include these sites or a secondary material that does include these moieties.

These initial materials studies were limited due to time and resources available—spanning from repetition of experiments and variation of the tested parameters. As these materials could face significantly more complex environments, additional definition of these environments and testing for such is required. With viscoelastic materials, the rate of loading of a force can have a significant impact on the behavior of the sample, which was qualitatively observed but not covered in full in these studies. Further characterization should also be conducted with respect to curing kinetics and the chemical evolution during UV exposure. Finally, though infrared was merely used as a qualitative analysis of a variation in the location of peaks experienced, it was not standardized and cannot be used to quantitatively measure any variation in absorbance and was not analyzed to identify key peaks. A hurdle in this analysis for this level of study was the lack of information on anticipated chemical functions in the material. Without the characteristic peaks identifiable, the infrared spectroscopy was not utilized to

its full potential. Moving forward, these are some of the most directly identifiable gaps in the research presented within this report.

With all materials covered in this set of studies, a serious requirement for further verification of application for cell-culture practices is the direct cell-culturing experimentation. Initial studies were conducted both on GelMA as formulated in the compression tests as well as on zein-based electrospun scaffolds, these were compromised due to a shift in accessibility of facilities. In order to best package these mechanical results, the cell-to-material interactions must be gauged, including protein assays, immunostaining, and long-term maturation studies. Though all components of the GelMA hydrogels have been tested heavily in cell culture and achieve high cell survivability, there are no studies done up to this point in which the soy-based resin has been tested for these types of applications. Similar materials have been tested for dental applications, but not for direct cellular environments and edible products. Once achieved, a more complete analysis of these materials can be deduced with respect to the question of their utility.

4.6 Conclusions

In this study, a GelMA hydrogel and a soybean oil-based degradable resin have been investigated for tissue engineering applications. Though GelMA contains an optimal environment to cells as it naturally contains RGD bonding moieties required for cell attachment, it can be difficult to achieve the desired mechanical strength or tailorability, typically at the cost of manufacturing accuracy or cell survivability. The soy-based resin was proven to have a higher mechanical resistance than that of GelMA and was

successfully degraded in biomaturation-related environments. A larger view of its behavior over a temperature range was built, which further helps to inform priorities in development and key constraints required to address in developing final consumable products to be sent to market.

As previously stated, these are not stand-alone answers to the mechanical or textural question with respect to cell cultured protein products. Textural imitation of meat tissue in cellular agriculture is still quite far from a reality. As an example, there is yet to be a consensus on the testing methodology that would be required to fully characterize the behavior, as well as the temperatures that are applicable to the products. The safety regulations are still in development for the emerging industry. The most likely answer to accomplishing a native tissue-like structure is through multi-material manufacturing. This multi-material approach could be tailored to different product needs, but the determination of the optimal properties is required before attempting to achieve them. Multi-materials may also require complex timings in processing to be successful, and will be highly dependent on what the goal of the products are. One argument in the cellular agriculture realm is whether these products need to imitate meat, or merely have the same nutritional profile or taste but otherwise be a different product altogether. It is the hope that in the next few years more answers on what success is and how to measure it will be developed in the field.

CHAPTER 5: SUMMARY, CONCLUSIONS, AND FUTURE WORK

5.1 Summary

In this work, an overview of cellular agriculture from a manufacturing and materials science point of view was provided, defining the opportunities for contributions therein. Focus on scale-up and texture was adopted to define the goal and objectives followed throughout these endeavors. One potential manufacturing process, DRUM, was proposed and multiple potential materials, GelMA and Biosoya1, were analyzed based upon food tissue engineering application requirements.

The DRUM system was developed and prototyped, including initial printability tests, followed by a discussion of the benefits and limitations of this platform for its use in tissue engineering or other multi-material manufacturing applications. GelMA was characterized using uniaxial compression and compared to that of native meat tissues, determining more testing would be required for full application verification and textural success. Finally, Biosoya1 resin was investigated over a range of temperatures and aging in degradation to further develop a baseline for understanding of the life of the product and the specific material behavior throughout.

5.2 Conclusions

Emphasis is made throughout this work that these are preliminary studies intended to forge a path forward in the convergence of multiple disciplines to solve the cellular agriculture question, and further the food horizon dilemma. As has been stated, these methods and materials are not fully investigated and would require significant additional characterizations before true implementation into this field can be completed.

Through these studies, it was determined that DRUM theoretically can function as an adjusted photolithographic manufacturing method to increase throughput of the system as a continuous production line. It also is modifiable to incorporate multiple materials. This can be realized with combinations of similar composition such as hydrogels containing different cell lines. Another potential multi-material method would incorporate different compositions like electrospun fibers to reinforce a hydrogel and improve mechanical resistance. The provided ability to change the orientation of the reinforcement layers may provide additional control in design of failure of these products when chewed and digested.

GelMA is a commonly-used hydrogel in biomedicine and contains the natural bonding sites for cell adhesion that is optimal for cell survivability during cell culture. However, GelMA is limited by the tailorability of the mechanical behavior it will exhibit under varied loadings. It is also material that is functionalized and animal-derived, which is counterproductive with respect to the development of animal-free animal products. Though this may not be a direct answer for the scaffold material for edible tissue engineering, its mechanical behavior is still very relevant to any gels that may be used in

these processes, synthetic or natural, and allows for development of methods while simultaneous work is being done in the development of materials.

Finally, it was shown that the biosoya, a soy-bean oil derived resin, was capable of being tailored to degrade, which reduced the moduli of the material towards what is expected of a raw meat product at that same texture. A significant drawback is the lack of cell-studies that was possible to be completed to ensure this material could be suitable for cell culture. This did allow, however, to develop a better framework for understanding of the requirements of cell-cultured protein products and the protocols required for verification.

5.3 Future Works

A very common motif throughout this work is that these are preliminary studies. Suggested future work is identified both in the development of this method itself as well as the development of a standard for this field. With respect to DRUM and the biomaterials used for photolithographic tissue engineering, additional testing of the printing resolution in the radial direction is required. There are two immediately identifiable hurdles in this endeavor. The first hurdle is the need for a projection pattern to be programmed to scroll at the same speed as the rotation of the collector. If this is not well-established, it can lead to accuracy errors between the intended and actual print. The second immediate hurdle to be faced in developing DRUM is the requirement to understand and utilize the fluid dynamics inherent in the system. This would involve in-depth studies and optimization both on the material to collector interactions as well as the viscosity and curing kinetics of the resin itself. These can all be directly influenced by

many factors such as ambient temperature and age of the material, which would need to be compensated for to achieve optimal results. Overall, this project moving forward will require the development of a team of individuals able to contribute to the optimization of separate components of the system.

In cellular biology or cellular agriculture, the research goals have been pretty well-defined by the community thus far. There is still much to do in terms of achieving the best cell lines and media for scale-up and sustainability. Textural understanding and replicability need to be further defined for these products as the standards for meat science is insufficient as conclusive standards to meet, due to the lack of in-depth information especially in thorough three-dimensional characterization. Many platforms for manufacturing these scaffolds or tissue products have been suggested in both industrial and academic research settings that need to be tested further for scaling and full applicability, such as thermal treatment effects. Tireless effort in continuing the process of defining FDA regulatory requirements and safety are needed. Last, but assuredly not least, full nutritional analyses and taste must be brought into consideration and standardized for all products.

With respect to the field of cellular agriculture as a whole, there is strong criticism against its potentiality for a more efficient food source, but regardless of it meeting its ultimate goal of disrupting traditional meat and dairy production many benefits have already been realized and many more anticipated on the horizon with the goal of environmental and fiscal improvements of cellular biology. It has shed light on often overlooked safety implications and stability concerns within the current food ecosystem. It questions preconceived notions on whether or not these traditions of practice are the

most suitable. Developments that otherwise may not have been discovered until decades from now in sustainability of cellular biology, such as animal-free media and others previously discussed, may in turn serve as a platform to reduce the costs of the expensive personalized medicine that is in development in tangent in the biomedicine and tissue engineering fields today. Even if cellular agriculture isn't the answer to the ultimate question for sourcing protein, it can provide significant innovation along the way to that conclusion.

REFERENCES

- [1] Milford AB, Le Mouël C, Bodirsky BL, Rolinski S. Drivers of meat consumption. *Appetite*. 2019;141:104313. <https://dx.doi.org/10.1016/j.appet.2019.06.005>. doi: 10.1016/j.appet.2019.06.005.
- [2] Stephens N, Di Silvio L, Dunsford I, Ellis M, Glencross A, Sexton A. Bringing cultured meat to market: Technical, socio-political, and regulatory challenges in cellular agriculture. *Trends in Food Science & Technology*. 2018;78:155-166. <https://dx.doi.org/10.1016/j.tifs.2018.04.010>. doi: 10.1016/j.tifs.2018.04.010.
- [3] Humbird D. Scale-up economics for cultured meat. *Biotechnology and bioengineering*. 2021;118(8):3239-3250. <https://onlinelibrary.wiley.com/doi/abs/10.1002/bit.27848>. doi: 10.1002/bit.27848.
- [4] How GMOS Are Regulated for Food and Plant Safety in the United States.
- [5] van Marle-Köster E, Visser C. Unintended consequences of selection for increased production on the health and welfare of livestock. *Archiv für Tierzucht*. 2021;64(1):177-185. <https://search.proquest.com/docview/2531494586>. doi: 10.5194/aab-64-177-2021.
- [6] Kaplan D. Integrated Approaches to Enhance Sustainability, Resiliency and Robustness in US Agri-food Systems. 2021;2021-69012-35978(\$10,000,000).
- [7] Reiley L. From lab to table: Will cell-cultured meat win over americans? *The Washington post*. May 3, 2019. Available from: <https://search.proquest.com/docview/2219392361>.
- [8] Ong KJ, Johnston J, Datar I, Sewalt V, Holmes D, Shatkin JA. Food safety considerations and research priorities for the cultured meat and seafood industry. *Comprehensive reviews in food science and food safety*. 2021;20(6):5421-5448. <https://onlinelibrary.wiley.com/doi/abs/10.1111/1541-4337.12853>. doi: 10.1111/1541-4337.12853.
- [9] Stout AJ, Mirliani AB, Rittenberg ML, et al. Simple and effective serum-free medium for sustained expansion of bovine satellite cells for cell cultured meat *Commun Biol*. 2022;5(1). doi: 10.1038/s42003-022-03423-8.
- [10] Cosenza Z, Astudillo R, Frazier P, Baar K, Block DE. Multi-information source bayesian optimization of culture media for cellular agriculture. *Biotechnology and bioengineering*. 2022. <https://www.ncbi.nlm.nih.gov/pubmed/35538846>. doi: 10.1002/bit.28132.
- [11] Yuen Jr JSK, Stout AJ, Kawecki NS, et al. Perspectives on scaling production of adipose tissue for food applications. *Biomaterials*. 2022;280:121273.

- <https://dx.doi.org/10.1016/j.biomaterials.2021.121273>. doi: 10.1016/j.biomaterials.2021.121273.
- [12] Campuzano S, Pelling AE. Scaffolds for 3D cell culture and cellular agriculture applications derived from non-animal sources. *Frontiers in sustainable food systems*. 2019;3. <https://doaj.org/article/12063334abe64ee78b2762d5c62d9f50>. doi: 10.3389/fsufs.2019.00038.
- [13] Furuhashi M, Morimoto Y, Shima A, Nakamura F, Ishikawa H, Takeuchi S. Formation of contractile 3D bovine muscle tissue for construction of millimetre-thick cultured steak *npj Sci Food*. 2021;5(1). doi: 10.1038/s41538-021-00090-7.
- [14] Alberts B, Johnson A, Lewis J, et al. Genesis, modulation, and regeneration of skeletal muscle. In: *Molecular biology of the cell*. New York: Garland Science; 2002. <https://www.ncbi.nlm.nih.gov/books/NBK26853/>.
- [15] Modifying matrix remodeling to prevent heart failure. 2014;41-60. doi: 10.1533/9780857096708.1.41.
- [16] Specht EA, Welch DR, Rees Clayton EM, Lagally CD. Opportunities for applying biomedical production and manufacturing methods to the development of the clean meat industry. *Biochemical engineering journal*. 2018;132:161-168. <https://dx.doi.org/10.1016/j.bej.2018.01.015>. doi: 10.1016/j.bej.2018.01.015.
- [17] Bellis SL. Advantages of RGD peptides for directing cell association with biomaterials. *Biomaterials*. 2011;32(18):4205-4210. <https://www.clinicalkey.es/playcontent/1-s2.0-S0142961211001815>. doi: 10.1016/j.biomaterials.2011.02.029.
- [18] Murphy CM, O'Brien FJ. Understanding the effect of mean pore size on cell activity in collagen-glycosaminoglycan scaffolds. *Cell adhesion & migration*. 2010;4(3):377-381. <https://www.tandfonline.com/doi/abs/10.4161/cam.4.3.11747>. doi: 10.4161/cam.4.3.11747.
- [19] Antoni D, Burckel H, Josset E, Noel G. Three-dimensional cell culture: A breakthrough in vivo. *International Journal of Molecular Sciences*. 2015;16(3):5517-5527. <https://www.ncbi.nlm.nih.gov/pubmed/25768338>. doi: 10.3390/ijms16035517.
- [20] Wang J, Wei Y, Zhao S, et al. The analysis of viability for mammalian cells treated at different temperatures and its application in cell shipment. *PLoS ONE*. 2017;12(4):e0176120. <https://www.ncbi.nlm.nih.gov/pubmed/28419157>. doi: 10.1371/journal.pone.0176120.

- [21] DuRaine GD, Brown WE, Hu JC, Athanasiou KA. Emergence of scaffold-free approaches for tissue engineering musculoskeletal cartilages. . 2015. <https://escholarship.org/uc/item/440901jk>.
- [22] Gershlak J, Hernandez S, Fontana G, et al. Crossing kingdoms: Using decellularized plants as perfusable tissue engineering scaffolds. *Biomaterials*. 2017;125:13-22. <https://www.clinicalkey.es/playcontent/1-s2.0-S0142961217300856>. doi: 10.1016/j.biomaterials.2017.02.011.
- [23] Yang G, Mun F, Kim G. Direct electrospinning writing for producing 3D hybrid constructs consisting of microfibers and macro-struts for tissue engineering. *Chemical engineering journal (Lausanne, Switzerland : 1996)*. 2016;288:648-658. <https://dx.doi.org/10.1016/j.cej.2015.12.047>. doi: 10.1016/j.cej.2015.12.047.
- [24] Nichol JW, Koshy ST, Bae H, Hwang CM, Yamanlar S, Khademhosseini A. Cell-laden microengineered gelatin methacrylate hydrogels. *Biomaterials*. 2010;31(21):5536-5544. <https://www.clinicalkey.es/playcontent/1-s2.0-S0142961210004485>. doi: 10.1016/j.biomaterials.2010.03.064.
- [25] Unagolla JM, Jayasuriya AC. Hydrogel-based 3D bioprinting: A comprehensive review on cell-laden hydrogels, bioink formulations, and future perspectives. *Applied materials today*. 2020;18:100479. <https://dx.doi.org/10.1016/j.apmt.2019.100479>. doi: 10.1016/j.apmt.2019.100479.
- [26] Lee J, Kim H. Emerging properties of hydrogels in tissue engineering. *Journal of Tissue Engineering*. 2018;9:2041731418768285. <https://journals.sagepub.com/doi/full/10.1177/2041731418768285>. doi: 10.1177/2041731418768285.
- [27] Yue K, Trujillo-de Santiago G, Alvarez MM, Tamayol A, Annabi N, Khademhosseini A. Synthesis, properties, and biomedical applications of gelatin methacryloyl (GelMA) hydrogels. *Biomaterials*. 2015;73:254-271. <https://www.clinicalkey.es/playcontent/1-s2.0-S014296121500719X>. doi: 10.1016/j.biomaterials.2015.08.045.
- [28] Bidarra SJ, Barrias CC, Fonseca KB, Barbosa MA, Soares RA, Granja PL. Injectable in situ crosslinkable RGD-modified alginate matrix for endothelial cells delivery. *Biomaterials*. 2011;32(31):7897-7904. <https://www.clinicalkey.es/playcontent/1-s2.0-S0142961211007848>. doi: 10.1016/j.biomaterials.2011.07.013.
- [29] Grigoryan B, Paulsen SJ, Corbett DC, et al. Multivascular networks and functional intravascular topologies within biocompatible hydrogels. *Science (American Association for the Advancement of Science)*. 2019;364(6439):458-464. <https://www.ncbi.nlm.nih.gov/pubmed/31048486>. doi: 10.1126/science.aav9750.

- [30] Lim KS, Schon BS, Mekhileri NV, et al. New visible-light photoinitiating system for improved print fidelity in gelatin-based bioinks. *ACS biomaterials science & engineering*. 2016;2(10):1752-1762. <http://dx.doi.org/10.1021/acsbiomaterials.6b00149>. doi: 10.1021/acsbiomaterials.6b00149.
- [31] Suresh G. Summarization of 3D-printing technology in processing & development of medical implants. *JOURNAL OF MECHANICS OF CONTINUA AND MATHEMATICAL SCIENCES*. 2019;14(1). doi: 10.26782/jmcmcs.2019.02.00012.
- [32] You F, Eames BF, Chen X. Application of extrusion-based hydrogel bioprinting for cartilage tissue engineering. *International Journal of Molecular Sciences*. 2017;18(7):1597. <https://www.ncbi.nlm.nih.gov/pubmed/28737701>. doi: 10.3390/ijms18071597.
- [33] Bencherif SA, Braschler TM, Renaud P. Advances in the design of macroporous polymer scaffolds for potential applications in dentistry. *Journal of periodontal & implant science*. 2013;43(6):251-261. <https://www.ncbi.nlm.nih.gov/pubmed/24455437>. doi: 10.5051/jpis.2013.43.6.251.
- [34] Aldana AA, Malatto L, Rehman MAU, Boccaccini AR, Abraham GA. Fabrication of gelatin methacrylate (GelMA) scaffolds with nano- and micro-topographical and morphological features. *Nanomaterials*. 2019;9(1):120. <https://www.ncbi.nlm.nih.gov/pubmed/30669422>. doi: 10.3390/nano9010120.
- [35] Xia H, Zhao D, Zhu H, et al. Lyophilized scaffolds fabricated from 3D-printed photocurable natural hydrogel for cartilage regeneration. *ACS applied materials & interfaces*. 2018;10(37):31704-31715. <http://dx.doi.org/10.1021/acsami.8b10926>. doi: 10.1021/acsami.8b10926.
- [36] Deng L, Zhang X, Li Y, et al. Characterization of gelatin/zein nanofibers by hybrid electrospinning. *Food hydrocolloids*. 2018;75:72-80. <https://dx.doi.org/10.1016/j.foodhyd.2017.09.011>. doi: 10.1016/j.foodhyd.2017.09.011.
- [37] Corey JM, Lin DY, Mycek KB, et al. Aligned electrospun nanofibers specify the direction of dorsal root ganglia neurite growth. *Journal of Biomedical Materials Research Part A*. 2007;83A(3):636-645. <https://api.istex.fr/ark:/67375/WNG-SFQBDL0S-J/fulltext.pdf>. doi: 10.1002/jbm.a.31285.
- [38] Vass P, Szabó E, Domokos A, et al. Scale-up of electrospinning technology: Applications in the pharmaceutical industry. *Wiley interdisciplinary reviews. Nanomedicine and nanobiotechnology*. 2020;12(4):e1611-n/a. <https://onlinelibrary.wiley.com/doi/abs/10.1002/wnan.1611>. doi: 10.1002/wnan.1611.

- [39] Zhao P, Gu H, Mi H, Rao C, Fu J, Turng L. Fabrication of scaffolds in tissue engineering: A review. *Front Mech Eng*. 2017;13(1):107-119. <https://link.springer.com/article/10.1007/s11465-018-0496-8>. doi: 10.1007/s11465-018-0496-8.
- [40] Wang X, Ding B, Li B. Biomimetic electrospun nanofibrous structures for tissue engineering. *Materials Today*. 2013;16(6):229-241. <https://dx.doi.org/10.1016/j.mattod.2013.06.005>. doi: 10.1016/j.mattod.2013.06.005.
- [41] Zhou Y, Chyu J, Zumwalt M. Recent progress of fabrication of cell scaffold by electrospinning technique for articular cartilage tissue engineering. *International Journal of Biomaterials*. 2018;2018:1953636-10. <https://dx.doi.org/10.1155/2018/1953636>. doi: 10.1155/2018/1953636.
- [42] Jing X, Li H, Mi H, Liu Y, Tan Y. Fabrication of fluffy shish-kebab structured nanofibers by electrospinning, CO₂ escaping foaming and controlled crystallization for biomimetic tissue engineering scaffolds. *Chemical engineering journal (Lausanne, Switzerland : 1996)*. 2019;372:785-795. <https://dx.doi.org/10.1016/j.cej.2019.04.194>. doi: 10.1016/j.cej.2019.04.194.
- [43] MacQueen LA, Alver CG, Chantre CO, et al. Muscle tissue engineering in fibrous gelatin: Implications for meat analogs. *NPJ science of food*. 2019;3(1):20. <https://www.ncbi.nlm.nih.gov/pubmed/31646181>. doi: 10.1038/s41538-019-0054-8.
- [44] Asmatulu R. Highly hydrophilic electrospun polyacrylonitrile/ polyvinylpyrrolidone nanofibers incorporated with gentamicin as filter medium for dam water and wastewater treatment. *Journal of Membrane and Separation Technology*. 2016;5(2):38-56. doi: 10.6000/1929-6037.2016.05.02.1.
- [45] Manji, Rizwan A., MD, PhD, MBA, FRCSC, Menkis, Alan H., DDS, MD, FRCSC, Ekser B, MD, Cooper, David K.C., MD, PhD, FRCS. Porcine bioprosthetic heart valves: The next generation. *The American heart journal*. 2012;164(2):177-185. <https://www.clinicalkey.es/playcontent/1-s2.0-S0002870312003675>. doi: 10.1016/j.ahj.2012.05.011.
- [46] Naso F, Gandaglia A. Different approaches to heart valve decellularization: A comprehensive overview of the past 30 years. *Xenotransplantation (København)*. 2018;25(1):e12354-n/a. <https://onlinelibrary.wiley.com/doi/abs/10.1111/xen.12354>. doi: 10.1111/xen.12354.
- [47] Adamski M, Fontana G, Gershlak JR, Gaudette GR, Le HD, Murphy WL. Two methods for decellularization of plant tissues for tissue engineering applications. *Journal of Visualized Experiments*. 2018(135). <https://www.jove.com/57586>. doi: 10.3791/57586.

- [48] Bayer A. Patent classification and information retrieval services. *Indexer*. 1981;12(3):117-124. <https://search.proquest.com/docview/1293717497>. doi: 10.3828/indexer.1981.12.3.2.
- [49] Allevi 2 bioprinter. <https://www.allevi3d.com/allevi-2/>.
- [50] Lumen X bioprinter. <https://www.cellink.com/bioprinting/lumen-x/>.
- [51] Holograph X bioprinter. . . <https://www.cellink.com/bioprinting/holograph-x/>.
- [52] Kelly BE, Bhattacharya I, Heidari H, Shusteff M, Spadaccini CM, Taylor HK. Volumetric additive manufacturing via tomographic reconstruction. *Science (American Association for the Advancement of Science)*. 2019;363(6431):1075-1079. <https://www.ncbi.nlm.nih.gov/pubmed/30705152>. doi: 10.1126/science.aau7114.
- [53] Dasgupta Q, Black 3, Lauren D. A FRESH SLATE for 3D bioprinting. *Science (American Association for the Advancement of Science)*. 2019;365(6452):446-447. <https://www.ncbi.nlm.nih.gov/pubmed/31371600>. doi: 10.1126/science.aay0478.
- [54] Peter R.N. Childs. Chapter 6 - rotating cylinders, annuli, and spheres. In: *Rotating flow*. Elsevier Inc; 2011:177-247. <https://dx.doi.org/10.1016/B978-0-12-382098-3.00006-8>. 10.1016/B978-0-12-382098-3.00006-8.
- [55] Dormer W, Gomes R, Meek MME, Directorate H, Canada H. Concise International Chemical Assessment Document 4 METHYL METHACRYLATE First draft prepared by MsWorld Health Organization Geneva. 1998.
- [56] Yue K, Trujillo-de Santiago G, Alvarez MM, Tamayol A, Annabi N, Khademhosseini A. Synthesis, properties, and biomedical applications of gelatin methacryloyl (GelMA) hydrogels. *Biomaterials*. 2015;73:254-271. <https://www.clinicalkey.es/playcontent/1-s2.0-S014296121500719X>. doi: 10.1016/j.biomaterials.2015.08.045.
- [57] Russell CS, Mostafavi A, Quint JP, et al. In situ printing of adhesive hydrogel scaffolds for the treatment of skeletal muscle injuries. *ACS applied bio materials*. 2020;3(3):1568-1579. <http://dx.doi.org/10.1021/acsabm.9b01176>. doi: 10.1021/acsabm.9b01176.
- [58] Labware chemical resistance table. chrome-extension://efaidnbmnnnibpcajpcglclefindmkaj/<https://tools.thermofisher.com/content/sfs/brochures/D20480.pdf>.
- [59] José C, Bonetto RD, Gambaro LA, et al. Investigation of the causes of deactivation–degradation of the commercial biocatalyst novozym® 435 in ethanol and ethanol–aqueous media. *Journal of molecular catalysis. B, Enzymatic*. 2011;71(3):95-107.








<https://dx.doi.org/10.1016/j.molcatb.2011.04.004>. doi:
10.1016/j.molcatb.2011.04.004.








- [60] Gaytán I, Burelo M, Loza-Tavera H. Current status on the biodegradability of acrylic polymers: Microorganisms, enzymes and metabolic pathways involved. *Appl Microbiol Biotechnol*. 2021;105(3):991-1006.
<https://link.springer.com/article/10.1007/s00253-020-11073-1>. doi: 10.1007/s00253-020-11073-1.
- [61] Paredes J, Cortizo-Lacalle D, Imaz AM, Aldazabal J, Vila M. Application of texture analysis methods for the characterization of cultured meat *Sci Rep*. 123456789;12(1). doi: 10.1038/s41598-022-07785-1.

APPENDIX

A1. Bill of Materials

Table A1-1. Rotating collector drum hardware system

Item:	URL:	Unit Cost:	Qty:	Total:
	1700 Series Face Tapped Stepper Motor Mount (NEMA 11) SKU: 1700-0016-0011	\$6.99	1	\$6.99
	1601 Series Flanged Ball Bearing (5mm ID x 14mm OD, 5mm Thickness) - 2 Pack SKU: 1601-0014-0005	\$2.99	1	\$2.99
	1121 Series Low-Side U-Channel (2 Hole, 72mm Length) SKU: 1121-0002-0072	\$2.39	1	\$2.39
	2100 Series Stainless Steel Round Shaft (6mm Diameter, 100mm Length) SKU: 2100-0006-0100	\$1.49	1	\$1.49
	1611 Series Flanged Ball Bearing (6mm ID x 14mm OD, 5mm Thickness) - 2 Pack SKU: 1611-0514-0006	\$2.99	1	\$2.99
	1500 Series Plastic Spacer (6mm ID x 8mm OD, 1mm Thickness) - 12 Pack SKU: 1500-0010-0006	\$1.99	1	\$1.99
	3401 Series Set Screw Round Belt Pulley (6mm Bore, 16mm PD) SKU: 3401-0006-0016	\$3.99	1	\$3.99

	3401 Series Set Screw Round Belt Pulley (5mm Bore, 16mm PD)	\$3.99	1	\$3.99
	SKU: 3401-0005-0016			
	1203 Series Block Mount (1-1) - 4 Pack	\$3.99	1	\$3.99
	SKU: 1203-0001-0001			
	1108 Series Flat Pattern Bracket (1-2)	\$1.79	2	\$3.58
	SKU: 1108-0001-0002			
	2906 Series Aluminum Set Screw Collar (6mm Bore, 8mm Length) - 2 Pack	\$2.49	2	\$4.98
	SKU: 2906-0006-0008			
	3405 Series Round Belt (5mm Cord Diameter, 95mm Circumference)	\$0.69	1	\$0.69
	SKU: 3405-0005-0095			
	2804 Series Zinc-Plated Steel Low Profile Socket Head Screw (M4 x 0.7mm, 8mm Length) - 25 Pack	\$1.89	1	\$1.89
	SKU: 2804-0004-0008			
	#1205 Stepper Motor: Bipolar, 200 Steps/Rev, 28x32mm, 3.8V, 0.67 A/Phase	15.95	1	\$15.95
	https://www.amazon.com/STEPPERONLINE-0-3-2-2A-10-30VDC-Micro-step-Resolutions/dp/B075R88FMN/ref=sr_1_1?keywo	27.5	1	\$27.50

rds=NEMA+11+stepper+motor+driver&qid=1582093139&sr=8-1			
https://www.grainger.com/product/POLYMERSH-APES-Rod-Stock-22JL38	18.5	1	\$18.50
Subtotal:			\$103.90

Table A.1-2 Components Purchased for coupling Collector (carriage and plate) and Main Structure

	Unit Cost:	Qty:	Total:
2812 Series Zinc-Plated Steel Nylon-Insert Locknut (M4 x 0.7mm, 7mm Hex) - 25 Pack	\$1.49	1	\$1.49
1600 Series Non-Flanged Ball Bearing (4mm ID x 10mm OD, 4mm Thickness) - 2 Pack	\$2.99	2	\$5.98
2800 Series Zinc-Plated Steel Socket Head Screw (M4 x 0.7mm, 50mm Length) - 25 Pack	\$3.79	1	\$3.79
https://www.mcmaster.com/91292a191	\$9.62	1	\$9.62
Subtotal:			\$20.88

Table A1-3 Components for Projection and main structural system

Item	Vendor	Part #	Cost
PRO6500, 405nm LED, 67mm Working Distance	Wintech Digital	PRO6500-405-01-67	\$9198.00
Clear acrylic, 0.22 inch (18"x24")	Lowe's	239981	\$48.96
Weld-on 4 Acrylic Adhesive	Amazon		\$15.00
mini-RAMBo 1.3	UltiMachine		\$128
Power supply	Amazon		\$10.99
Linear Actuator	THK	TSM11Q-2RM-002	\$715.00
Aluminum Extrusion Frame	Misumi	HFSB5-2040-350	\$19.32
Nut for Aluminum Extrusion	Misumi	HNKK5-5	\$21.25
32mm Star Head M8x20 Male Thread Screw	NewEgg	9SIA27C3KH6046	\$12.27
gorilla double-sided mounting tape	Amazon		\$6.74

Plastic-head thumb screws (pkg qty 10)	McMaster-Carr	96016A062	\$5.50
M2.5x10 (pkg Qty 100)	McMaster-Carr	91292A014	\$5.42
M3 nuts (pkg qty 25)	McMaster-Carr	92497A200	\$17.14
M3x8 (Pkg qty 100)	McMaster-Carr	91292A112	\$4.52
M3x12 (pkg qty 100)	McMaster-Carr	91292A114	\$4.97
M5x6 (pkg qty 50)	McMaster-Carr	91292A189	\$5.23
Mirror 2"x2", 12-piece	Amazon		\$11.99
	Total without projector		\$1,032.30
	Total with projector		\$10,230.30

Table A1-4 Calculated Totals

Table/Component	Cost
A1-1	\$103.90
A1-2	\$20.88
A1-3 (not including projector)	\$1032.30
Projector	\$9198.00
Total (no Projector)	\$1,157.08
Total (with Projector)	\$10,355.08

A2. Code

The following is the Arduino code developed to control the rotational collector drum:

```
#include "AccelStepper.h"
#include "Wire.h"

#define ELECTRONICS "RAMBo13a"

#define X_STEP_PIN    37
#define X_DIR_PIN     48
#define X_ENABLE_PIN  29

#define L_STEP_PIN    72
#define L_DIR_PIN     50
```

```

#define L_ENABLE_PIN      29

#define MOTOR_CURRENT_PWM_XY_PIN 46
#define X_MS1             40
#define X_MS2             41
#define LED_PIN           13

#define THERMO            3

AccelStepper stepperR(1, X_STEP_PIN, X_DIR_PIN); // 1 = Driver
AccelStepper stepperL(1, L_STEP_PIN, L_DIR_PIN); // 2 = Driver

// Interrupt pin parameters
const byte interruptPin = 18;
#define GND 19
#define VCC 84
volatile byte state = LOW;
int count = 0;

// Variables to keep track of the timing of recent interrupts
unsigned long button_time = 0;
unsigned long last_button_time = 0;

// Serial parameters and user values to change
long incomingByte = 0; // for incoming serial data
long rollSpeed = 500;
long linearSpeed = 4000;
long layerHeight = 200;
long partThickness = 100;
String inString = ""; // string to hold input

void setup()
{
  Serial.begin(9600);

  // Limit switch setup
  pinMode(interruptPin, INPUT_PULLUP);
  pinMode(GND, OUTPUT);
  pinMode(VCC, OUTPUT);
  digitalWrite(GND, LOW);
  digitalWrite(VCC, HIGH);
  attachInterrupt(digitalPinToInterrupt(interruptPin), limit, CHANGE);

  // Drive setup for linear
  // Enables linear actuator motor

```

```

pinMode(THERMO, OUTPUT);
digitalWrite(THERMO, HIGH);

stepperL.setMaxSpeed(4000);
stepperL.setAcceleration(100);

stepperL.setEnablePin(L_ENABLE_PIN);
stepperL.setPinsInverted(false, false, true); //invert logic of enable pin
stepperL.enableOutputs();

// Drive setup for rolling
// Sets PWM power to rolling stepper
analogWrite(46,64);

// Sets the controller to 1/8 microstepping
pinMode(X_MS1, OUTPUT);
pinMode(X_MS2, OUTPUT);
digitalWrite(X_MS1, HIGH);
digitalWrite(X_MS2, HIGH);

stepperR.setMaxSpeed(4000);
stepperR.setAcceleration(100);

stepperR.setEnablePin(X_ENABLE_PIN);
stepperR.setPinsInverted(false, false, true); //invert logic of enable pin
stepperR.enableOutputs();
}

void loop()
{
  Serial.println("Hello!");
  Serial.println("Please choose one of the following.");
  Serial.println("Type Home (1), Start (2), SetRSpeed (3), Pull Out of Resin (7)");
  // send data only when you receive data:
  while(true)
  {
    while (Serial.available() > 0)
    {
      // read the incoming byte:
      incomingByte = Serial.read();

      switch (incomingByte)
      {
        case '1':
          Serial.println("Setting Home. Please wait.");
          linear();

```

```
Serial.println("Done!");
break;
case '2':
Serial.println("Starting the print.");
stepperR.setSpeed(rollSpeed);
while (true)
{
stepperR.runSpeed();
}
Serial.println("Printing jobs is done!");
break;
case '3':
Serial.println("Set the rotational speed.");
readMonitor();
rollSpeed = incomingByte;
Serial.print("Rotational speed set to: ");
Serial.println(rollSpeed);
break;
case '4':
Serial.println("Set the linear actuator speed.");
readMonitor();
linearSpeed = incomingByte;
Serial.print("Linear actuator speed set to: ");
Serial.println(linearSpeed);
break;
case '5':
Serial.println("Set the number of layers in-between solidification.");
readMonitor();
layerHeight = incomingByte;
Serial.print("Layer number set to: ");
Serial.println(layerHeight);
break;
case '6':
Serial.println("Set the thickness of the wall to print.");
readMonitor();
partThickness = incomingByte;
Serial.print("Part thickness set to: ");
Serial.println(partThickness);
break;
case '7':
Serial.println("Pulling out of resin");
linear2();
Serial.println("Done!");
break;
default:
break;
```

```

    }
    Serial.println("Please choose one of the following.");
    Serial.println("Type Home (1), Start (2), SetRSpeed (3), Pull Out of Resin (7)");
  }
}

// Limit switch method.
void limit()
{
  button_time = millis();
  //check to see if increment() was called in the last 25 milliseconds
  if (button_time - last_button_time > 25)
  {
    state = !state;
    last_button_time = button_time;
  }
}

// Reads the serial monitor of the Arduino IDE for user inputs.
void readMonitor()
{
  while(true)
  {
    if (Serial.available() > 0)
    {
      int inChar = Serial.read();
      if (isDigit(inChar))
      {
        // convert the incoming byte to a char and add it to the string:
        inString += (char)inChar;
      }
      // if you get a newline, print the string, then the string's value:
      if (inChar == '\n' && inString.toInt() != 0)
      {
        Serial.println(inString.toInt());
        incomingByte = inString.toInt();
        inString = "";
        return;
      }
    }
  }
}

// Drives linear stepper motor step by step at given speed. (20000 step/rev)
void linear()

```

```

{
  long k = linearSpeed;
  linearSpeed = -4000;
  stepperL.setSpeed(linearSpeed);
  while (state == false)
  {
    stepperL.runSpeed();
  }
  linearSpeed = 1000;
  stepperL.setSpeed(linearSpeed);
  while (state == true)
  {
    stepperL.runSpeed();
  }
  linearSpeed = k;
}

```

// Drives linear stepper motor step by step at given speed. (20000 step/rev)

```

void linear2()
{
  stepperL.setCurrentPosition(0);
  stepperL.moveTo(100000);
  stepperL.setSpeed(4000);
  boolean runs = true;
  while (runs)
  {
    if (stepperL.distanceToGo() > 0)
    {
      stepperL.runSpeedToPosition();
    }
    else
    {
      runs = false;
    }
  }
}

```

// Drives rotational stepper motor step by step at given speed. (200 step/rev)+1/8

```

microstepped
void printing()
{
  stepperR.setCurrentPosition(0);
  stepperR.moveTo(3200);
  stepperR.setSpeed(rollSpeed);
  stepperL.setCurrentPosition(0);
  stepperL.moveTo(layerHeight);
}

```

```
stepperL.setSpeed(linearSpeed);
boolean runs = true;
while (runs)
{
  if (stepperR.distanceToGo() > 0 || stepperL.distanceToGo() > 0)
  {
    stepperR.runSpeedToPosition();
    stepperL.runSpeedToPosition();
  }
  else
  {
    runs = false;
  }
}

// Unused
void runsss()
{
  for (int x = 0; x < partThickness; x++)
  {
    printing();
  }
  stepperL.setCurrentPosition(0);
  stepperL.moveTo(60000);
  stepperL.setSpeed(4000);
  boolean runss = true;
  while (runss)
  {
    if (stepperL.distanceToGo() > 0)
    {
      stepperL.runSpeedToPosition();
    }
    else
    {
      runss = false;
    }
  }
}
```